

KERNFORSCHUNGSZENTRUM

KARLSRUHE

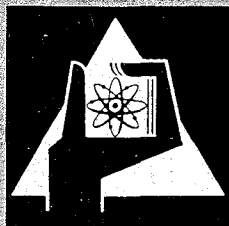
April 1969

KFK 724
EUR 4178 e

Institut für Reaktorentwicklung

Temperature Distribution and Thermal Stability
in Asymmetrical Triangular Rod-Clusters

M. Fischer, H. Shimamune



GESELLSCHAFT FÜR KERNFORSCHUNG M. B. H.

KARLSRUHE

KERNFORSCHUNGSZENTRUM KARLSRUHE

April 1969

KFK 724

EUR 4178e

Institut für Reaktorentwicklung

Temperature Distribution and Thermal Stability in

Asymmetrical Triangular Rod-Clusters ¹⁾

by

M.Fischer and H.Shimamune ²⁾

Gesellschaft für Kernforschung m.b.H., Karlsruhe

- 1) Work performed within the association in the field of fast reactors between the European Atomic Energy Community and Gesellschaft für Kernforschung m.b.H., Karlsruhe.
- 2) On delegation from Japan Atomic Energy Research Institute Tokai Mura, Japan.

Abstract

Theoretical analysis is presented on fluid flow and heat transfer for axial turbulent flow in asymmetrical triangular rod-clusters caused by thermal bowing or fabrication inaccuracies. The method is applicable to calculate distribution of local shearing stress, coolant velocity, coolant temperature and local surface temperature. It can be used to the stability of bowed fuel rods and to decide the proper spacing of the supports. Numerical results are obtained for steam cooled fuels by eddy diffusivity and arc depth of bowing as parameters. Theoretical considerations are also applicable to sodium coolant.

Table of Contents

Abstract

I.	Introduction	1
II.	Geometry and Assumption	3
III.	Flow Velocity Distribution	5
IV.	Force Balance Equation	7
V.	Heat Balance Equation	11
VI.	Thermal Bowing	16
VII.	Discussion of Numerical Results	18
VIII.	Conclusion	21
	Nomenclature	23
	References	27
	Tables	30
	Figures	

I. Introduction

Every fuel rod is suffered from bowing to some extent because of tolerances in manufacturing and asymmetrical distribution of temperature around the rods that develops during operation. Initial bowing will cause a change of the hydraulic and thermal conditions around the rods which result in a change of the temperature distribution, increasing the initial rod bowing until balanced conditions will be reached.

Since the effect of thermal bowing has direct and strong influences on the hot channel conditions [1] and core design it must be thoroughly analysed in detail. In the present work such deviated fuel rod-bundles, which we call "asymmetrical rod clusters", are investigated.

There seems to be no work so far that treated asymmetrical rod-clusters but A.C.Rapier and T.M.Jones [2]. However, they considered neither asymmetrical triangular rod arrangement nor actual supporting conditions in an accurate manner. It is a well known fact that the effect of rod-cluster geometry becomes very large when p/d values are in the range of 1.3 and smaller. In this region, simplified models of geometry can not be used, instead of actual ones. For example, the eccentric annular model gives too high heat transfer coefficients. So far, this problem has not been investigated, and no paper has been presented.

There are several papers published on a symmetrical geometry. The first theoretical treatment is the work done by R.G.Deissler and M.F.Taylor [3]. Major disadvantages of their work come from the fact that no considerations were made to shearing stress and flow mixing. O.D.Dwyer [4.5.6] developed an ingenious method to improve these disadvantages. In his method, flow mixing in the peripheral directions is already included, although no consideration is given to the shearing stress. Dwyer's model is indeed a direct expression of intuitive observation to the physical phenomena, but his method

seems to be too time consuming and not to be applicable to the asymmetrical geometry.

A.C.Rapier and J.D.Redman [7,8] investigated analytically the flow distribution in symmetrical rod clusters using correlations for the eddy diffusivity of moment which were based on their own experiments. However, they discussed only the flow velocity distribution, not the temperature distribution. R. Nijsing, I.Gargantini and W. Eifler [9] used in their analysis the same type of segment as A.C. Rapier and J.D.Redman in the force balance equation, but they adopted Blasius's correlation and Elder's correlation for the shearing stress and eddy diffusivity of momentum respectively, [10]. They pointed out that in proceeding the analysis in the way to subdivide a channel into many segments as they adopted, there must be a contradiction between mathematical and physical requirements. Therefore, they introduced a model of subchannel elements which satisfies both, mathematical and physical requirements.

In this paper, a new method to calculate the coolant velocity distribution in the triangular rod cluster is presented in Section III and IV. In the symmetrical cluster-geometry, one has only to consider one element of subchannels. But in case of the asymmetrical rod-arrangement, the mathematical treatment is much more complicated because of the complex interrelations between all channel - elements, as shown in this paper. In Section V, the temperature distribution in the coolant and the cladding on the rod circumferences is calculated under the assumption that the eddy diffusivity of heat is equal to the eddy diffusivity momentum. In Section VI, fuel rod bowing is discussed by using the results obtained in the preceding sections. Unless each supporting point is fixed rigidly, the effect caused by the adjoining parts of the span in question can not be neglected. The supporting method adopted in this paper is the four points method, that admits displacement only in the axial direction.

II. Geometry and Assumptions

The fuel assembly to which the analysis is applied consists of triangular rod-clusters. However, one rod deviates from its normal position by the angle $\Theta = 30$ degree and the distance δ . Each fuel rod has neither fins nor promoters. The geometrical and other parameters are listed in Table 1.

The sub-channels are divided into twelve elements around the rod. These elements are again divided into a number of segments. Each segment is bounded by the rod wall, two radial velocity-gradient-lines and the maximum-velocity-line.

To avoid the contradiction between mathematical and physical requirements, as R.Nijsing pointed out, in the present work a new method is developed. It seems to be rather difficult to apply Nijsing's method to the present model of asymmetrical geometry, because of the following two reasons. Firstly, higher order terms must be included to simulate satisfactorily the shape of the elements. Nijsing selected four terms in his calculation, but the discrepancy could not be neglected. In the "Law of Wall" that gives the distribution of generalized flow velocity, the distance between the wall and the point under consideration is the important parameter. If the law is applied, the shape of the element should not be modified to a considerable extent, because the flow distribution would change even though the flow rate and the element area remain constant (see Fig.2). Secondly, it is very complicated and difficult to define properly the maximum velocity line which satisfies all boundary conditions between the elements used in this method.

In the present paper, therefore, a new and simpler method is developed (Fig.3). Each original, straight maximum velocity -line is replaced by two modified curves, a straight line SR and a circular arc RN. The radius of the circular arc RN is determined by a simple calculation if only the length C is specified. According to this method, the discrepancy between mathematical and physical requirements can be eliminated. Furthermore, this method does not affect

the flow distribution essentially and can be applied to asymmetrical as well as to symmetrical geometries. The area of the element becomes slightly smaller by the amount of area NQR (see Fig.3). The difference, however, becomes smaller as the radius of the arc becomes shorter, and for the numerical calculation the difference could be made negligibly small. Adopting this model, the problem turns to be an initial value problem of non-linear differential equation. Since there is no general way to get exact analytical solution the method was applied assuming an initial value for each segment. The equation shows strong instability, so the selection of initial value must be as accurate as possible.

Following assumptions are made in performing the analysis:

1. For fully developed turbulent flow, the axial temperature gradient dT/dx is independent of the angular coordinate φ .
2. Density ρ , specific heat capacity C_p , dynamic viscosity μ_d , are constant in a segment. These parameters are functions of the average temperature in the segment.
3. The pressure is constant in the cross-sectional area of the sub-channel.
4. For steam as coolant, the eddy diffusivity of heat ϵ_H can be chosen equal to the eddy diffusivity of momentum ϵ_M . For sodium as coolant the relation $\epsilon_H \sqrt{Na} = 0.6 \epsilon_M \sqrt{\text{Steam}}$ (see Section VI), which is based on experiments [21], is assumed to be approximately valid.
5. The heat flux is constant for large eddy diffusivity values, but a modified cosine distribution is taken for small eddy diffusivities.
6. No exchange of heat and momentum across the maximum velocity lines a-b-c-d-e-f (Fig.1)
7. The coolant flow is steady.
8. The resultant circumferential flow velocity u_φ and resultant radial flow velocity u_r are zero.
9. The coolant is incompressible.
10. The power density is uniform in the cross-sectional area of the fuel.

III. Flow Velocity and Distribution

According to the experiments with tubes and parallel plates, it is well known that the relation between generalized velocity and generalized distance in the turbulent flow can be expressed by the following correlation,

$$u^+ = A + B \ln y^+ \quad (3-1)$$

where

$$u^+ = u/u^* \quad (3-2)$$

$$y^+ = y u^* \rho / \mu \quad (3-3)$$

$$u^* = \sqrt{\tau_w / \rho} \quad (3-4)$$

In the present analysis, we assume that the profile of the generalized velocity can be expressed by only this equation and do not consider about laminar sublayer and transition zone. Kármán [11] gave the value 5.5 and 2.5 respectively to the constants A and B. We assume that the correlation (3-1) holds in each segment of our model. The average generalized velocity in a segment at a given angular coordinate is given by

$$\bar{u}^+ = \frac{\bar{u}}{u^*} = \frac{\int_{r_0}^{r_0+\hat{y}} u^+ \cdot \left(\frac{d}{2} + y\right) dy}{\int_{r_0}^{r_0+\hat{y}} \left(\frac{d}{2} + y\right) dy} \quad (3-5)$$

$$\bar{u}^+ = A - B + B \ln \left(\frac{\hat{y} \rho u^*}{\mu} \right) + \frac{B}{2} \left(\frac{\hat{y}}{d + \hat{y}} \right)$$

In the new model, one element composes of two smaller elements, i.e., element A and element B. Then there are also two types of segments, i.e., the one which belongs to element A and the other which belongs to element B (see Fig.3).

The segments which belong to element A have the following hydraulic parameters:

Length of segment:

$$\hat{y} = \frac{1}{2} (p \sec \varphi - d) \quad (3-6)$$

Cross-sectional area:

$$dS = \int_{r_0}^{r_0 + \hat{y}} r dr = \frac{1}{2} (d + \hat{y}) \hat{y} d\varphi \quad (3-7)$$

Equivalent hydraulic diameter:

$$d_e = 4 \frac{dS}{r_0 d\varphi} = 4 \left(1 + \frac{\hat{y}}{d}\right) \hat{y} \quad (3-8)$$

The segments which belong to element B have the following parameters:

Length of segment:

$$\hat{y} = \left(\frac{P}{2 \cos H} - C - R\right) \cos \varphi \quad (3-9)$$

$$+ \sqrt{\left(\frac{P}{2 \cos H} - C - R\right)^2 \cos^2 \varphi - \left(\frac{P}{2 \cos H} - C\right)^2 + 2 \left(\frac{P}{2 \cos H} - C\right) R - \frac{d}{2}}$$

where C is given arbitrarily, but recommended to be as small as possible. H and R are fixed, if the deviated length f , deviated angle Θ and C are specified.

Cross-sectional area:

$$dS = \int_{r_0}^{r_0 + \hat{y}} r dr = \frac{1}{2} (d + \hat{y}) \hat{y} d\varphi \quad (3-10)$$

Equivalent hydraulic diameter:

$$d_e = 4 \frac{dS}{r_0 d\varphi} = 4 \hat{y} \left(1 + \frac{\hat{y}}{d}\right) \quad (3-11)$$

IV. Force Balance Equation

The Navier-Stoke's equation for incompressible fluid

$$\frac{\partial \tau}{\partial t} + (\tau \nabla) \tau = - \frac{1}{\rho} \text{grad } P + \frac{\mu}{\rho} \Delta \tau \quad (4-1)$$

is expressed in the cylindrical coordinates r, φ, x as follows

$$\begin{aligned} & \frac{\partial u_r}{\partial t} + u_r \frac{\partial u_r}{\partial r} + u_\varphi \frac{\partial u_r}{r \partial \varphi} + u_x \frac{\partial u_r}{\partial x} - \frac{u_\varphi^2}{r} \\ & = - \frac{1}{\rho} \frac{\partial P}{\partial r} + \frac{\mu}{\rho} \left(\frac{\partial^2 u_r}{\partial r^2} + \frac{1}{r^2} \frac{\partial^2 u_r}{\partial \varphi^2} + \frac{\partial^2 u_r}{\partial x^2} + \frac{1}{r} \frac{\partial u_r}{\partial r} - \frac{2}{r^2} \frac{\partial u_\varphi}{\partial \varphi} - \frac{u_r}{r^2} \right) \\ & \frac{\partial u_\varphi}{\partial t} + u_r \frac{\partial u_\varphi}{\partial r} + u_\varphi \frac{\partial u_\varphi}{r \partial \varphi} + u_x \frac{\partial u_\varphi}{\partial x} + \frac{u_r u_\varphi}{r} \\ & = - \frac{1}{\rho} \frac{\partial P}{\partial \varphi} + \frac{\mu}{\rho} \left(\frac{\partial^2 u_\varphi}{\partial r^2} + \frac{1}{r^2} \frac{\partial^2 u_\varphi}{\partial \varphi^2} + \frac{\partial^2 u_\varphi}{\partial x^2} + \frac{1}{r} \frac{\partial u_\varphi}{\partial r} + \frac{2}{r^2} \frac{\partial u_r}{\partial \varphi} - \frac{u_\varphi}{r^2} \right) \\ & \frac{\partial u_x}{\partial t} + u_r \frac{\partial u_x}{\partial r} + u_\varphi \frac{\partial u_x}{r \partial \varphi} + u_x \frac{\partial u_x}{\partial x} \\ & = - \frac{1}{\rho} \frac{\partial P}{\partial x} + \frac{\mu}{\rho} \left(\frac{\partial^2 u_x}{\partial r^2} + \frac{1}{r^2} \frac{\partial^2 u_x}{\partial \varphi^2} + \frac{\partial^2 u_x}{\partial x^2} + \frac{1}{r} \frac{\partial u_x}{\partial r} \right) \end{aligned} \quad (4-2)$$

Continuity

$$\text{div } \tau = 0 \quad (4-3)$$

or

$$\frac{\partial u_r}{\partial t} + \frac{1}{r} \frac{\partial u_\varphi}{\partial \varphi} + \frac{\partial u_x}{\partial x} + \frac{u_r}{r} = 0 \quad (4-4)$$

with the assumptions, $u_r = 0, u_\varphi = 0, \partial u_x / \partial t = 0$ one obtains from eqs. (4-2) and (4-4)

$$\frac{1}{\rho} \frac{\partial}{\partial r} \left(r \mu \frac{\partial u}{\partial r} \right) + \frac{1}{\rho} \frac{\partial}{\partial \varphi} \left(\mu \frac{\partial u}{r \partial \varphi} \right) = \frac{1}{\rho} \frac{\partial P}{\partial x} \quad (4-5)$$

where u is substituted for u_x . Here, $\mu \frac{\partial u}{\partial r}$ is a shearing stress which acts on the circumferential plane, and $\frac{\mu}{r} \frac{\partial u}{\partial \varphi}$ is a shearing stress which acts on the radial plane. In a turbulent flow, shearing stress is composed of the shearing stress induced by molecular viscosity and the shearing stress occurring from the exchange of momentum, i.e., Reynolds stress. J. Boussinesq [12] first suggested that the Reynolds stress could be expressed as follows

$$\bar{\tau}_t = \rho \epsilon_M \frac{\partial u}{\partial y}$$

Thus the shearing stress on circumferential and radial planes, respectively, can be written in the following form

$$\begin{aligned} \tau_r &= \mu \frac{\partial u}{\partial r} \\ &= (\mu_d + \rho \epsilon_{M_t}) \frac{\partial u}{\partial r} \end{aligned} \quad (4-6)$$

and

$$\begin{aligned} \bar{\tau}_\varphi &= \mu \frac{\partial u}{r \partial \varphi} \\ &= (\mu_d + \rho \epsilon_{M_\varphi}) \frac{\partial u}{r \partial \varphi} \end{aligned} \quad (4-7)$$

Then from eqs.(4-5) it follows

$$\frac{\partial (r \bar{\tau}_r)}{\partial r} + \frac{\partial \bar{\tau}_\varphi}{\partial \varphi} = \frac{\partial P}{\partial x} r \quad (4-8)$$

Integrating from the wall surface to the maximum-velocity-line it follows

$$\begin{aligned} \int_{r_0}^{r_0 + \hat{y}} \frac{\partial (r \bar{\tau}_r)}{\partial r} dr + \int_{r_0}^{r_0 + \hat{y}} \frac{\partial \bar{\tau}_\varphi}{\partial \varphi} dr &= \frac{dP}{dx} \int_{r_0}^{r_0 + \hat{y}} r dr \\ (r_0 + \hat{y}) \bar{\tau}_r \Big|_{r=r_0 + \hat{y}} - r_0 \bar{\tau}_w + \frac{\partial}{\partial \varphi} \int_{r_0}^{r_0 + \hat{y}} \bar{\tau}_\varphi dr &= \frac{1}{2} \frac{dP}{dx} (d + \hat{y}) \hat{y} \end{aligned}$$

On the maximum-velocity-line, there is no shearing stress, $\tau_y \Big|_{r=r_0+y} = 0$ therefore it holds

$$r_0 \bar{\tau}_w = -\frac{1}{2} \frac{dP}{dx} (d+y) \bar{y} + \frac{\partial}{\partial y} \int_{r_0}^{r_0+y} \bar{\tau}_y dr \quad (4-9)$$

To solve this equation, we must introduce further changes. From the equation (4-7) one obtains

$$\bar{\tau}_y = (\mu_d + \rho \epsilon_{M\varphi}) \frac{\partial u}{r \partial y} = \frac{(\mu_d + \rho \epsilon_{M\varphi})(u^+ + B)}{r} \frac{\partial u^+}{\partial y}$$

In a fully developed turbulent flow, the effect of the dynamic viscosity is negligibly small compared with the effect of the eddy viscosity, $\rho \epsilon_{M\varphi}$. The constant B(=2.5) might also be neglected compared with u^+ (≈ 30). With this the following equation results.

$$\bar{\tau}_y = \frac{\rho \epsilon_{M\varphi}}{r} u^+ \frac{\partial u^+}{\partial y} \quad (4-10)$$

The selection of the correlation or value for $\epsilon_{M\varphi}$ is one of the most important considerations. In the present analysis, Rapier's correlation [8] multiplied by a constant factor F was selected, because this correlation is convenient for analysis.

$$\epsilon_{M\varphi} = F \frac{u^+ \bar{y}}{10} \quad (4-11)$$

Table 2 shows the experimental results and semi-empirical correlation which were obtained by previous researchers, normalized to Rapier's results. According to Table 2, Rapier's correlation gives the minimum value compared with the other investigations. The coefficient F was taken to 1 for the calculation of the shearing stress distribution, and F=1, 3.47, 13.4 and 57 for the calculation of the temperature distribution.

Sandborn [13] showed that the eddy diffusivity is almost independent from the distance of the various points in the channel to the wall except at the vicinity of the wall. Therefore, we assume that the eddy diffusivity is independent from the radial distance r. Hence, it follows

$$\int_{r_0}^{r_0 + \hat{y}} \tau_{\varphi} dr = \frac{F}{5} \frac{\hat{y}^2}{d + \hat{y}} \xi \bar{u}^+ u^* \frac{\partial u^*}{\partial \varphi}$$

Substituting this expression to eq.(4-9), and introducing the relation $\tau_w = \xi u^{*2}$, one obtains

$$\xi \tau_0 u^{*2} = - \frac{dP}{dx} \frac{dS}{d\varphi} + \frac{F}{5} \frac{\partial}{\partial \varphi} \left(\frac{\hat{y}^2}{d + \hat{y}} \xi \bar{u}^+ u^* \frac{\partial u^*}{\partial \varphi} \right)$$

If we put

$$\phi_1 = 5 \frac{dP}{dx} \frac{dS}{d\varphi} / F$$

$$\phi_2 = 5 \xi \tau_0 / F$$

$$\phi_3 = \frac{\hat{y}^2}{d + \hat{y}}$$

then the following differential equation results

$$\frac{\partial^2 u^*}{\partial \varphi^2} = \frac{1}{\phi_3 \xi \bar{u}^+} \left(\frac{\phi_1}{u^*} + \phi_2 u^* \right) - \left(\frac{1}{\phi_3} \frac{\partial \phi_3}{\partial \varphi} + \frac{1}{\xi} \frac{\partial \xi}{\partial \varphi} + \frac{1}{\bar{u}^+} \frac{\partial \bar{u}^+}{\partial \varphi} \right) \frac{\partial u^*}{\partial \varphi} - \frac{1}{u^*} \left(\frac{\partial u^*}{\partial \varphi} \right)^2 \quad (4-12)$$

This differential equation can be solved by numerical method.

Boundary condition

$$\frac{\partial u^*}{\partial \varphi} = 0 \quad \text{at} \quad \varphi = 0, \pi \quad (4-13)$$

$$u^* \Big|_{\substack{i=1 \\ j=J}} = u^* \Big|_{\substack{i=N \\ j=J-1}} \quad \begin{matrix} i = 1, \dots, N \\ j = 1, \dots, J \end{matrix} \quad (4-14)$$

$$\frac{\partial u^*}{\partial \varphi} \Big|_{\substack{i=1 \\ j=J}} = \frac{\partial u^*}{\partial \varphi} \Big|_{\substack{i=N \\ j=J-1}} \quad (4-15)$$

V. Heat Balance Equation

The heat balance equation applied for the differential fluid element showed in Fig.4 is expressed as follows in cylindrical coordinates,

$$-\frac{\partial}{\partial r} \left\{ (\lambda + \beta g c_p \epsilon_{Hr}) r \frac{\partial T}{\partial r} \right\} - \frac{\partial}{\partial \varphi} \left\{ (\lambda + \beta g c_p \epsilon_{H\varphi}) r \frac{\partial T}{\partial \varphi} \right\} + \frac{\partial}{\partial x} (u + \beta g c_p T) = 0 \quad (5-1)$$

Integrating from r_0 to $r_0 + \hat{y}$ it follows

$$-\left. (\lambda + \beta g c_p \epsilon_{Hr}) r \frac{\partial T}{\partial r} \right|_{r=r_0+\hat{y}} + \left. (\lambda + \beta g c_p \epsilon_{Hr}) r \frac{\partial T}{\partial r} \right|_{r=r_0} - \frac{\partial}{\partial \varphi} \int_{r_0}^{r_0+\hat{y}} (\lambda + \beta g c_p \epsilon_{H\varphi}) \frac{\partial T}{\partial \varphi} \frac{dr}{r} + \frac{\partial}{\partial x} \int_{r_0}^{r_0+\hat{y}} u \beta g c_p T r dr = 0$$

However, in this equation the first term is equal to 0, and the second term is equal to $-q \cdot r_0$.

If we further assume that $\lambda, \beta, c_p, \epsilon_{Hr}, \epsilon_{H\varphi}, T$ and u are mean values in a channel-segment, the following relation results.

$$q = \frac{1}{d} \frac{\partial}{\partial x} \left\{ u \beta g c_p T (d + \hat{y}) \hat{y} \right\} - \frac{1}{r_0} \frac{\partial}{\partial \varphi} \left\{ (\lambda + \beta g c_p \epsilon_{H\varphi}) \frac{\partial T}{\partial \varphi} \ln \left(1 + \frac{\hat{y}}{r_0} \right) \right\} \quad (5-2)$$

We consider a short distance along the axial direction and assume that u, β, c_p and \hat{y} are independent of the axial coordinate x ,

$$q(\varphi) = \frac{1}{d} (d + \hat{y}) \hat{y} u \beta g c_p \frac{\partial T}{\partial x} - \frac{1}{r_0} \frac{\partial}{\partial \varphi} \left\{ (\lambda + \beta g c_p \epsilon_{H\varphi}) \ln \left(1 + \frac{\hat{y}}{r_0} \right) \frac{\partial T}{\partial \varphi} \right\} \quad (5-3)$$

If the coolant is steam, the effect of the thermal conductivity λ is negligible compared with the thermal diffusivity $\epsilon_{H\varphi}$. For fully developed turbulent flow, the following heat balance holds

$$\frac{\partial T(\varphi, x)}{\partial x} = \frac{q_{av} \pi d}{u_0 s_0 c_p s_0 z} \quad (5-4)$$

where subscript 0 means the average value in a subchannel. For steam as coolant, we can assume that same correlation holds for both, the thermal eddy diffusivity and the momentum eddy diffusivity according to eq.(4-11)

$$\epsilon_{H\varphi} = F \frac{u^* \hat{y}}{10} \quad (5-5)$$

For the sodium as coolant, we can make use of the result which has been obtained by K.G.Eickhoff et al., [21]. They determined experimentally the ratio of the eddy diffusivity of mass in air, $\epsilon_M(\text{air})$, to the eddy diffusivity of heat in sodium, $\epsilon_H(\text{Na})$, and got the result of $\epsilon_H / \epsilon_M = 0.6 \pm 0.1$ in the range of Reynolds numbers of $2 \div 6 \times 10^4$. Thus, in the case of sodium we use the relation

$$\epsilon_{H\varphi} = 0.6 \cdot F \frac{u^* \hat{y}}{10} \quad (5-6)$$

but now it is not allowed to neglect the effect of the thermal conductivity in eq.(5-3).

In this paper we investigate steam as coolant. Then eq.(5-3) becomes

$$q(\varphi) = q_{av} \frac{c_p \gamma}{u_0 c_{p0} s_0} \frac{\partial e}{\partial e} \bar{u} + u^* - \frac{F \cdot g}{10 s_0} \frac{\partial}{\partial \varphi} \left\{ \hat{y} s_{cp} u^* \ln \left(1 + \frac{\hat{y}}{r_0} \right) \frac{\partial T}{\partial \varphi} \right\} \quad (5-7)$$

Here we must consider the heat flux distribution on the rod circumference. In the case of symmetrical geometry and at relatively large value of p/d , or large thermal diffusivity, it may be allowed to assume that the heat flux is constant. But when the mixing effect is small or the effect of eccentricity becomes large, this assumption raises some contradiction, i.e., though the heat generation density and heat flux are uniform, the temperature difference between the hot and cold side of the rod becomes very large. Because it is a very complicated

problem at the actual asymmetrical geometry to obtain the heat flux distribution by an exact, analytical method, we assume a modified cosine distribution. This distribution is based on the cosine function and added by higher harmonics

$$q(\varphi) = q_{av} \frac{\left\{ 1 - E \left(\cos \varphi + \frac{1}{2} \cos 2\varphi - \frac{1}{2} \right) \right\}}{\left(1 + \frac{E}{2} \right)} \quad (5-8)$$

where E is a parameter defining the shape of the heat flux distribution. ($0 \leq E \leq 1$).

With the assumption of uniform power density, some amount of heat should flow inside the rod from the hot to the cold side due to the temperature difference, i.e.,

$$\begin{aligned} \Delta Q &= 2 \int_0^{\varphi_b} (q_{av} - q(\varphi)) r_0 d\varphi \\ &= d \cdot q_{av} \left[\varphi_b - \frac{\left\{ \varphi_b - E \left(\sin \varphi_b + \frac{1}{4} \sin 2\varphi_b - \frac{1}{2} \varphi_b \right) \right\}}{\left(1 + \frac{E}{2} \right)} \right] \end{aligned} \quad (5-9)$$

where φ_b is the angular coordinate at $q(\varphi) = q_{av}$.

As a first approximation we estimate the temperature difference, ΔT_f , which is necessary to induce the flow of ΔQ inside the rod by using a simplified model instead of treating the actual geometry (see Fig.5).

$$\Delta T_f = \frac{d}{(2 \lambda_c t + \lambda_u d_u)} \Delta Q \quad (5-10)$$

This temperature difference, ΔT_f , must be equal to the temperature difference of the wall surface ΔT_w , which is obtained from the coolant temperature distribution according to eq.(5-12),

$$\Delta T_f = \Delta T_w \quad (5-11)$$

We can find out the optimum values by graphical method taking E as parameter. First, for several assumed values of E, we calculate the temperature distribution of coolant and clad surface from the

equations (5-12) (5-18), and then obtain the temperature difference between the hot side and the cold side of the rod surface, ΔT_w . On the other side, we draw the curve which shows the necessary temperature difference, ΔT_f , to induce the flow of ΔQ inside the rod itself taking E as parameter. The crossing point of these two curves give the optimum values of E .

If we put in eq.(5-7)

$$\Psi_1 = \frac{C_p \gamma}{u_0 \varphi_0 \gamma_0} \frac{de}{De}$$

$$\Psi_2 = C_p \gamma F$$

$$\Psi_3 = \frac{\gamma^2}{d + \hat{\gamma}}$$

$$\Psi_4 = \left\{ 1 - E \left(\cos \varphi + \frac{1}{2} \cos 2\varphi - \frac{1}{2} \right) \right\} / \left(1 + \frac{E}{2} \right)$$

$$G_1 = 5 \tau_0 q_{av}$$

the following differential equation results

$$\frac{\partial^2 T}{\partial \varphi^2} = \frac{G}{\Psi_2 \Psi_3} \left(\Psi_1 \bar{u}^+ - \frac{\Psi_4}{u^*} \right) - \left(\frac{1}{3} \frac{\partial \beta}{\partial \varphi} + \frac{1}{C_p} \frac{\partial C_p}{\partial \varphi} + \frac{1}{u^*} \frac{\partial u^*}{\partial \varphi} + \frac{1}{\Psi_3} \frac{\partial \Psi_3}{\partial \varphi} \right) \frac{\partial T}{\partial \varphi} \quad (5-12)$$

This is the equation to be solved.

Boundary conditions

$$\frac{\partial T}{\partial \varphi} = 0 \quad \text{at } \varphi = 0, \pi \quad (5-13)$$

$$T \Big|_{\substack{i=1 \\ j=J}} = T \Big|_{\substack{i=N \\ j=J-1}} \quad i = 1, \dots, N \quad (5-14)$$

$$\frac{\partial T}{\partial \varphi} \Big|_{\substack{i=1 \\ j=J}} = \frac{\partial T}{\partial \varphi} \Big|_{\substack{i=N \\ j=J-1}} \quad j = 1, \dots, 6 \quad (5-15)$$

Moreover, to arrive at the solution of eq.(5-12) we need the

conservation of energy

$$\sum_{i=1}^n \bar{u} \rho g c_p (T - T_0) ds = 0 \quad (5-16)$$

The local heat transfer coefficient is assumed to be defined by the following correlation according to [22]

$$\begin{aligned} h &= 0.0197 \frac{\lambda}{d_e} (Re)^{0.82} (Pr)^{0.4} \\ &= 0.0197 \lambda^{0.6} \mu^{-0.42} c_p^{0.4} d_e^{-0.18} \rho^{0.82} \bar{u}^{0.82} \end{aligned} \quad (5-17)$$

After the elimination of \bar{u} one obtains

$$h = 0.0197 \rho^{0.4} \left(\frac{2}{f} \frac{dP}{dx} \right)^{0.41} \lambda^{0.6} c_p^{0.4} d_e^{0.23} \rho^{0.41} \mu_d^{-0.42} \quad (5-18)$$

VI. Thermal bowing

In the preceding Sections, the circumferential distribution of clad temperature in a closely packed fuel rod cluster has been analysed as function of actual cooling and heat transfer conditions in the reactor-core. If the temperature distribution on the rod circumference is not symmetrical, then the temperature difference between the hot and the cold side, ΔT_w , will induce thermal bowing of the fuel rod.

In this Section the relation between the temperature difference and the deflection of the rods from the standpoint of the strength of the material will be obtained, i.e., the temperature difference, ΔT_n , which is necessary to induce a specified deflection under a given supporting distance will be analysed. If ΔT_n is larger than ΔT_w for the same value of deflection, then the bowing phenomenon is stable.

The following assumptions are involved in the analysis:

1. Power density keeps uniform after bowing occurred.
2. The temperature difference between the hot and the cold side of the fuel rod is constant all over the distance between two supports.

The differential equation of the bended rod which receives the temperature difference is expressed by

$$\frac{d^2 f}{dx^2} = \frac{1}{\rho_t} + \frac{1}{\rho_b} \quad (6-1)$$

where ρ_t is the radius of curvature which is induced by thermal expansion when the fuel rod is exposed to the temperature difference $\Delta T_w = (T_{wo} - T_{wi})$, in the free support condition,

$$\frac{1}{\rho_t} = \frac{\alpha \Delta T_w}{d} \quad (6-2)$$

and ρ_b is the radius of curvature induced by loads acting on the supporting points. The absolute values of these loads are decided from the condition that the resultant deflection at the supporting points must be zero.

Generally, the temperature distribution around the wall can be expressed by the Fourier series,

$$T_w(\varphi) = \bar{T}_w + \sum_1^{\infty} (A_n \cos n\varphi + B_n \sin n\varphi)$$

The mean value, \bar{T}_w , produces uniform axial and circumferential expansion of the clad. Since essentially only the first harmonic of T_w causes local curvature of the rod, and since the temperature distribution becomes symmetrical to the diameter at $\theta = 30^\circ$, one obtains

$$T_w(\varphi) = \bar{T}_w + \frac{1}{2} (T_{w0} - T_{wi}) \cos n\varphi$$

The circumferential temperature distribution of the clad surface, $T_w(\rho)$, depends on the deviation length of the rod f , and it should be therefore also a function of axial coordinate x . However, it is assumed as a first approximation that ρ_t is constant between two supports and its value is taken at the most deviated position. This simplifies the problem and leads to a safety-sided evaluation.

Bending curve caused by temperature difference

The deviations induced by the temperature difference only are given by the following equations (Fig.6b).

$$A \sim B \quad f^* = \frac{lx}{2\sqrt{\rho_t^2 - (\frac{l}{2})^2}} - \frac{\beta l^2}{2\sqrt{\rho_t^2 - (\frac{l}{2})^2}} \quad (6-3)$$

$$B \sim M \quad f^* = \sqrt{\rho_t^2 - \left\{ \left(\frac{l}{2} + \beta x \right) - x \right\}^2} - \sqrt{\rho_t^2 - \left(\frac{l}{2} \right)^2} \quad (6-4)$$

Bending curve caused by loads

The deflections induced by the loads W_a , W_b , W_c and W_d ($W_a = W_b = W_c = W_d$) acting on the supporting points (Fig.6c) are

$$A \sim B \quad f^{**} = \frac{W_A}{EJ} \left[\frac{1}{6} \left\{ x^3 - 3\left(\beta l + \frac{l}{2}\right)^2 x + 2\left(\beta l + \frac{l}{2}\right)^3 \right\} - \frac{1}{6} \left\{ -\left(\frac{l}{2}\right)^3 + 3\left(\frac{l}{2}\right)^2 \left(\beta l + \frac{l}{2}\right) - 3\left(\frac{l}{2}\right)^2 x \right\} - \frac{\beta l^3}{8} \right] \quad (6-5)$$

$$B \sim M \quad f^{**} = \frac{W_A}{EJ} \left[\frac{1}{6} \left\{ x^3 - 3\left(\beta l + \frac{l}{2}\right)^2 x + 2\left(\beta l + \frac{l}{2}\right)^3 \right\} - \frac{1}{6} \left\{ (x - \beta l)^3 - 3\left(\frac{l}{2}\right)^2 (x - \beta l) + 2\left(\frac{l}{2}\right)^3 \right\} - \frac{\beta l^3}{8} \right] \quad (6-6)$$

W_a is fixed by the condition that the resultant deviation at supporting point A equals to zero.

$$W_A = \frac{\frac{\beta l^2}{2St}}{\left\{ \frac{(2\beta+1)^3}{24} - \frac{(3\beta+1)}{24} - \frac{\beta}{8} \right\} \frac{l^3}{EJ}} \quad (6-7)$$

The resultant deviation at x is, then, given by adding these two components (Fig.6a),

$$f = f^* + f^{**} \quad (6-8)$$

If we put $\beta = 1$, the deviation length at $x = \beta l + l/2$ i.e., the maximum deviation is given as follows

$$f = \frac{7}{40} \frac{\alpha l^2}{d} \Delta T_w \quad (6-9)$$

VII. Discussion of Numerical Results

The analytical procedure outlined in the preceding Sections has been applied to a numerical example. The fundamental parameters are given in Table 1.

ξ , M_d and c_p are assumed constant in the cross-sectional area of coolant channel.

Fig. 7 shows the distribution of the local friction velocity on the circumference of the deviated fuel rod at various deviations f .

Fig. 8 shows the distribution of mean flow velocity in a segment around the deviated fuel rod. In the symmetrical case ($p/d = 1.16$), the ratio of the maximum velocity to the minimum velocity is about 1.2, but if thermal bowing occurs this ratio increases remarkably and reaches as large as 5 in the case of $f = 1$ mm.

Fig. 9-16 show the temperature distribution of coolant and clad surface, T and T_w respectively, versus angular coordinate φ , using the deviation f as parameter. As we can see in the figures, the effect of eddy diffusivity is very large. For example in the case of a relatively large deviation, $f = 0.6$ mm. In this case, the maximum temperature difference ΔT_w is only 15°C for $F = 57$, but it reaches already 340°C for $F = 1$. Because there is up to now no reasonable knowledge about the diffusivity with respect to the problems of this work, we treated the eddy diffusivity as parameter and calculated the curves for $F = 1, 3.47, 13.4$ and 57 . $F = 1$ corresponds to Rapier's correlation [8] and gives the minimum value among the collected data. $F = 3.47$ corresponds to Kattchee's correlation [19] and Moyer [20] also used this correlation to carry out his analysis $F = 13.4$ is the mean value of the collected data, and $F = 57$ is the maximum value of the data.

The temperature difference ΔT_w grows very sharply with the growth of the deviation length f . Considering the case of $F = 13.4$ for example, ΔT_w is only 7°C for $f = 0.2$ mm, 17.4°C for $f = 0.4$ mm, but increasing rapidly with the increase of f , i.e., becomes 39.4°C for $f = 0.6$ mm, 81°C for $f = 0.8$ mm and reaches up to 184°C for $f = 1$ mm. All curves show that the temperatures of the coolant and of the rod wall become high level only in the first channel-element ($\varphi = 0; \pi/6$) and decrease sharply in the second element. Comparing all cases, one recognizes that there exist great differences in the temperature level in the first channel according to each f and F values, but not so remarkable differences are present in the other channel-elements. From these results, we can recognize that the thermal bowing has a strong effect on the hot channel situation.

In the first channel element ($\psi = 0 \div \pi/6$), the coolant temperature keeps almost uniform level, but the clad temperature shows a peak near the $\psi = \pi/6$, i.e., hot spot.

From the figures 10, 12, 14 and 16, we can draw the curves which show the relation between temperature difference of fuel clad ΔT_w and the deviated length f through the parameter F (Fig.17). The dotted lines show the temperature difference of fuel clad ΔT_n , necessary to induce the specified deviation for the given supporting distance e . For a certain deviation length f , if $\Delta T_w > \Delta T_n$, this asymmetrical layout is stable. But if $\Delta T_n < \Delta T_w$, i.e., in the area of right side of crossing point, the asymmetrical layout is unstable, and the deviation may increase more and more until touch with the neighbouring fuel rods.

Fig. 18 shows the relation between the deviation length f and supporting distance e . The upper side of each curve is unstable area, and the lower side is stable area. Following are examples how to see this figure.

	$l = 10 \text{ cm}$	$l = 15$	$l = 20$
$F = 1$	$f < 0.36 \text{ mm}$ stable > unstable	$f < 0.02$ stable > unstable	always unstable always unstable
$F = 3.47$	$f < 0.84$ stable > unstable	$f < 0.5$ stable > unstable	$f < 0.22$ stable > unstable
$F = 13.4$	$f < 1$ stable > unstable	$f < 0.96$ stable > unstable	$f < 0.73$ stable > unstable
$F = 57$	always stable	always stable	always stable

As shown in the examples, the analysis developed in this work provides the proper supporting distance ℓ for prospecting values of deviation ξ .

VIII. Conclusions

The analysis presented in this work predicts the distribution of the coolant flow velocity, the temperature distribution of the coolant and the cladding and proper supporting distances in the important cases of asymmetrical triangular fuel-rod-clusters. With respect to an early practical approach, several assumptions and approximations were unavoidable, but these simplifications are reasonably well safety-sided.

The results show that if thermal rod bowing occurs, the velocity and temperature distribution in the rod cluster will change considerably. This is an important phenomenon with regard to the thermal-hydraulic core design and to reactor safety. Therefore, the design of a compact fuel assembly, with a small p/d value and a high power density, must be analysed thoroughly not only with regard to the nominal symmetrical geometry but even more to the always presented asymmetrical geometry of the hot channel as described in this work.

There are some problems which have arisen during the course of the work and which need further investigation.

1. Eddy diffusivity:

To arrive at the real flow and temperature distribution in the rod cluster, the eddy diffusivities of momentum and heat claim the primary concern in the analysis. It is, therefore, most important to select proper data of these factors which are applicable to the actual conditions. However, there are rather large differences

Nomenclature

A	=	Constant in eq.(3-1), normally taken to be 5.5
B	=	Constant in eq.(3-1), normally taken to be 2.5
C	=	Length defined in Fig.3
<hr/>		
C_1	=	Constant in eq.(5-12)
c_p	=	Specific heat of fluid at constant pressure, Kcal/(Kp°C)
d	=	Outer diameter of clad, m
d_u	=	Diameter of fuel, m
D_e	=	Equivalent hydraulic diameter of subchannel, m
E	=	1. Young's modulus 2. Parameter of heat flux distribution
f	=	Friction factor
F	=	Coefficient of eddy diffusivity
g	=	Gravity acceleration, m/s ²
h	=	Local heat transfer coefficient, Kcal/(m ² s°C)
l	=	Axial distance between two supports, m
I	=	Second moment of area of fuel cross-section
p	=	Pitch of fuel rod, m
p_0	=	Pitch of fuel rod for symmetrical geometry, m
p	=	Static pressure, at
p_r	=	Prandtl number = $(c_p \mu g) / \lambda$
q	=	Heat flux of fuel rod, Kcal/(s m ²)
q_{av}	=	Average heat flux of fuel rod, Kcal/(s m ²)
R	=	Radius defined in Fig.3
Re	=	Reynolds number in symmetrical subchannel = $(D_e u_0 g) / \mu$
r	=	Radial distance in cylindrical coordinate, m
r_0	=	Radius of fuel rod = $d/2$, m

- S = Cross-sectional area of subchannel in symmetrical geometry, m^2
- dS = Cross-sectional area of segment, m^2
- T = Coolant temperature, $^{\circ}C$
- T_w = Clad temperature, $^{\circ}C$
- T_k = Clad temperature, $^{\circ}K$
- ΔT_w = ~~Temperature difference of clad surface between the hot side and the cold side, $^{\circ}C$~~
- ΔT_f = Temperature difference of clad surface between the hot side and the cold side defined by eq.(5-10), $^{\circ}C$
- ΔT_n = Temperature difference of clad surface between the hot side and the cold side defined by eq.(6-9), $^{\circ}C$
- t = 1. Clad thickness, m
2. Time, s
- u = Local flow velocity, m/s
- \bar{u} = average flow velocity in a segment, m/s
- u^+ = Generalized flow velocity = u/u^*
- \bar{u}^+ = average generalized flow velocity = \bar{u}/u^*
- u^* = Friction velocity = $\sqrt{\tau_w / \rho}$, m/s
- \bar{u}^* = Mean value of u^* around the circumference of the wall, m/s
- u_0 = Average flow velocity in the symmetrical geometry, m/s
- v = Specific volume of coolant, m^3/Kp
- x = Axial coordinate, m
- y = Perpendicular distance from rod wall, m
- y^+ = Generalized distance from rod wall
- \hat{y} = Radial distance from wall to maximum-velocity-line, m
- \hat{y}^+ = Generalized radial distance from wall to maximum-velocity-line
- W = Load acting at supporting point, Kp/m^2
- α = Coefficient of linear thermal expansion of clad
- β = Coefficient of supporting distance
- γ = Specific weight of coolant, Kp/m^3

- d_e = Equivalent hydraulic diameter of segment, m
- ϵ_M = Eddy diffusivity of momentum, m^2/s
- ϵ_H = Eddy diffusivity of heat, m^2/s
- Θ = Angular coordinate of deviations, Degree
- H = Angle defined in Fig.3, rad
-
- λ = Thermal conductivity of coolant, $Kcal/(m\ s^\circ C)$
- λ_c = Thermal conductivity of clad, $Kcal/(m\ s^\circ C)$
- λ_u = Thermal conductivity of fuel, $Kcal/(m\ s^\circ C)$
- μ = Coefficient of shear stress, $(Kp.s)/m^2$
- μ_d = Dynamic viscosity, $(Kp\ s)/m^2$
- ν = Kinematic viscosity, m^2/s
- f = Length of deviation, m
- ρ = 1. Coolant density, Kg/m^3 , $(Kp\ s^2)/m^4$
2. Radius of curvature of fuel rod, m
- ρ_b = Radius of curvature induced by loads, m
- ρ_t = Radius of curvature induced by temperature difference, m
- τ_r = Fluid shear stress on circumferential plane, Kp/m^2
- τ_φ = Fluid shear stress on radial plane, Kp/m^2
- τ_w = τ_r at rod wall, Kp/m^2
- τ_o = τ_w in symmetrical geometry, Kp/m^2
- φ = Angular coordinate of a segment, rad
- ϕ_1 = Function defined in eq.(4-12)
- ϕ_2 = Function defined in eq.(4-12)
- ϕ_3 = Function defined in eq.(4-12)
- ψ_1 = Function defined in eq.(5-12)
- ψ_2 = Function defined in eq.(5-12)
- ψ_3 = Function defined in eq.(5-12)
- ψ_4 = Function defined in eq.(5-12)

Subscripts

i = Number of segment

j = Number of channel-element

0 = Average value in a symmetrical geometry

r = Radial direction

φ = Circumferential direction

References

1. M. Fischer; Die Heißkanalfaktoren dampfgekühlter Reaktoren, Internal Report Nuclear Research Center Karlsruhe (1966).
2. A.C.Rapiers and T.M.Jones; Thermal Bowing of Reactor Fuel Elements, Journal of Nuclear Energy, Part A/B, Reactor Science and Technology, 1965, Vol.19, pp 145-191
3. R.G.Deissler and M.F.Taylor; Analysis of Axial Turbulent Flow and Heat Transfer, TID 7529
4. O.E.Dwyer; Analytical Study of Heat Transfer to Liquid Metals Flowing In-line Through Closely Packed Rod Bundles. Nuclear Science and Engineering, Vol.25, 1966, pp 343-358
5. W.S.Yu and O.E.Dwyer; Heat Transfer to Liquid Metals Flowing Turbulently in Eccentric Annuli - I, Nuclear Science and Engineering.
6. W.S.Yu and O.E.Dwyer; Heat Transfer to Liquid Metals Flowing Turbulently in Eccentric Annuli - II, Nuclear and Engineering, Vol.27, P.1-9, 1967.
7. A.C.Rapiers and J.D. Redman; Calculation of Velocity Distributions in Rod Clusters, Journal Mechanical Engineering Science, Vol.7, No.4, p.460-468.
8. A.C.Rapiers; Forced Convection Heat Transfer in Passages with varying Roughness and Heat Flux around the Perimeter, Proc. Intn. Mech.Engrs., London, 1963-64.

9. R.Nijsing, I.Gargantini and W.Eifler; Analysis of Fluid Flow and Heat Transfer in a Triangular Array of Parallel Heat Generating Rods, Nuclear Engineering and Design, Vol.4, No.4, p.375-398, 1966.
10. J.W.Elder; The Dispersion of Marked Fluid in Turbulent Shear Flow, Journal of Fluid Mechanics, No.5, 1959.
11. T.V.Kármán; Trans.ASME, 61, 705, 1939.
12. J.Boussinesq; Theorie de l'Ecoulement Tourbillonnant, Paris, 1897.
13. V.A.Sandborn; Experimental Evaluation of Momentum Terms in Turbulent Pipe Flow. Nat.Aero. Space Admin.Tech., Note 3266, Jan., 1955
14. R.D.Collins and J.France; Mixing of Coolant in Channels between Close-Packed Fuel Elements, UKAEA, Research and Development Branch, Capenhurst, IGR-TN/CA-847, Jan., 1958.
15. A.A.Bishop, et al.; Thermal and Hydraulic Design of the CVTR Fuel Assemblies, Topical Report, Westinghouse Electric Corp., Atomic Power Division, CVNA-115, June, 1962
16. P.A.Nelson, et al.; Mixing in Flow Parallel to Rod Bundles Having a Square Lattice, Westinghouse Electric Corp., Atomic Power Division, WCAP-1607, July, 1960.
17. E.D.Waters; Fluid Mixing Experiments with a Wire-Wrapped 7-Rod Bundle Fuel Assembly, General Electric Corp., Hanford Atomic Products Operation, HW-70178, Aug., 1961.

18. W.H.Bell and B.W.Le Tourneau; Experimental Measurements of Mixing in Parallel Flow Rod Bundles, Westingshouse Electric Corp., WAPD-TH-381, 1958.
19. N.Kattchee and W.C.Reynolds; Hectic II-An IBM 7090 Fortran Computer Program for Heat Transfer Analysis of Gas of Liquid Cooled Reactor Passages, Aerojet-General Nucleonics, IDO-28595, Dec., 1962.
20. C.B.Moyer; Coolant Mixing in Multi-Rod Fuel Bundles, Riso Report No.125, July, 1964, DOR Design Study, Copenhagen.
21. K.J.Eickhoff, J.Alen and C.Boormann; Engineering Development for Sodium System, London Conference on Fast Breeder Reactors, Ref: 5B/5, May, 1966.
22. R. Nijsing; Diffusion Phenomena associated with Transfer of Momentum, Heat and Mass in Turbulent Pipe Flow, EUR 293 E, 1963.

Table 1

Parameter		Symbol	Values selected for numerical calculation	
Coolant	Reynolds number	R_e	2.64×10^5	
	temperature (average)	T	500	[°C]
	static pressure	P	180	[at]
	friction factor	f	0.02	
	material		steam	
Clad.	outer diameter	d	7	[mm]
	thickness	t	0.37	[mm]
	thermal conductivity	λ_c	0.19	[W/cm·c]
	coefficient of linear thermal expansion	α	1.15×10^{-5}	
	material		Inconel 6.25	
Fuel	diameter	d_u	6.26	[mm]
	heat flux (average)	q_{av}	354	[kW/m ² s]
	power	Q	0.464	[MW/l]
	thermal conductivity	λ_u	0.024	[W/cm ^o C]
	material		UO ₂ (80%)-PO ₂ (20%)	
Pitch length (symmetrical)	P_o		8.15	[mm]
Geometry			triangle layout	

Table 2

Reference	Equation	Fluid	$\epsilon \times 10^4 \frac{m^2}{s}$	Normalized value = F	
Collins	[14]	experiment	Air	114	57
Bishop	[15]	"	Water	64.4	32.2
Nelson	[16]	"	"	29.4	14.7
Waters	[17]	"	"	10.4	5.2
Bell	[18]	"	"	6.8	3.4
"	"	"	"	4.52	2.26
Kattchee	[19]	$\frac{Re}{20} \sqrt{\frac{F}{2}} \cdot v$	Steam	6.95	3.47
Elder	[10]	$0.0115 Re^{7/8} v$	"	3.36	1.68
Rapier	[8]	$u^* \gamma / 10$	"	2	1
Average				26.8	13.4

[note] The last two values in the fourth column are calculated applying the present data to the equations of Elder and Rapier. Other values are calculated from the ratio of observed value to the predicted value using Kattchee's equation. A list of the ratio is given in Moyer's report [20].

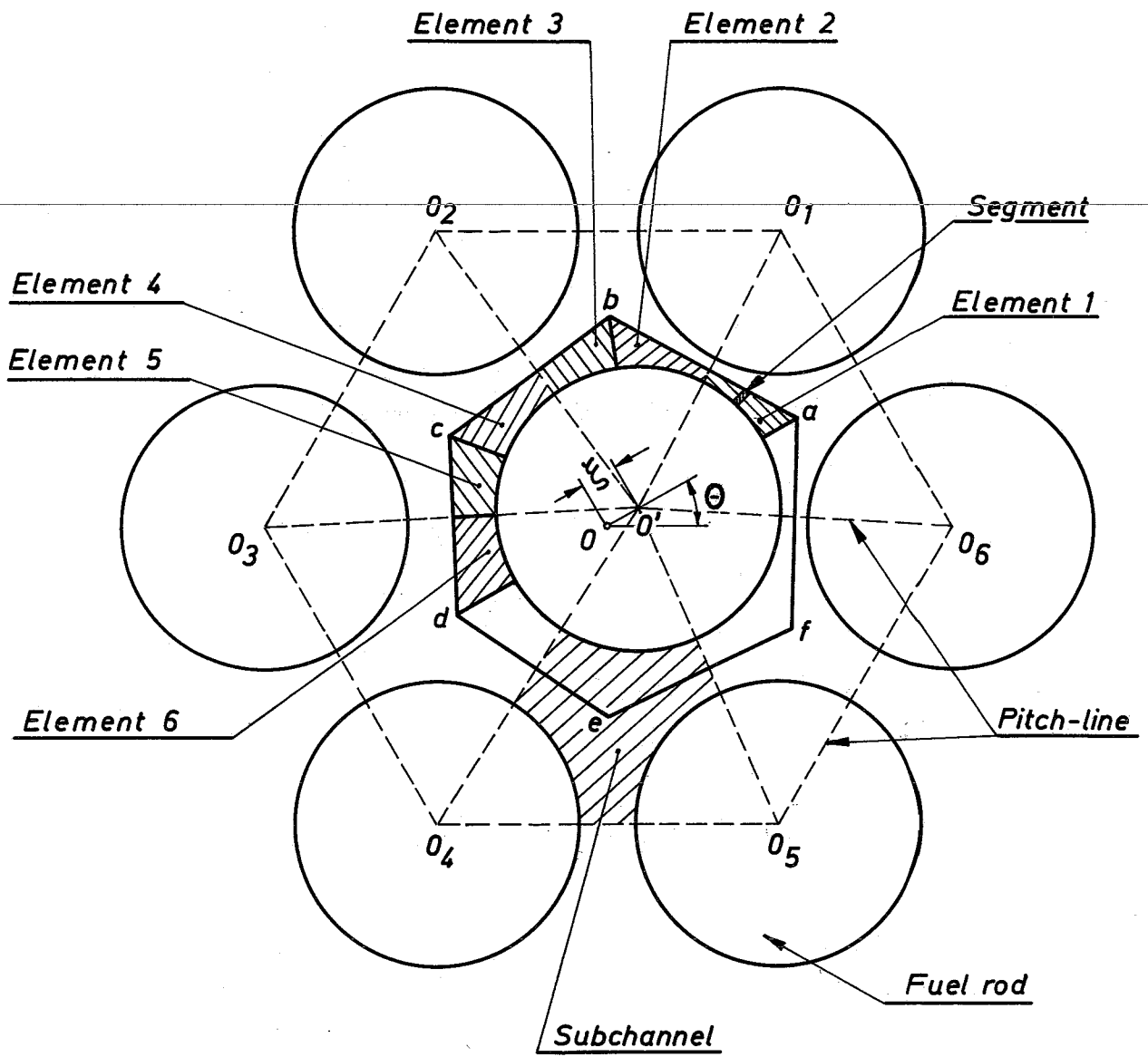


Fig.1 Cross-section of asymmetrical triangular rod clusters

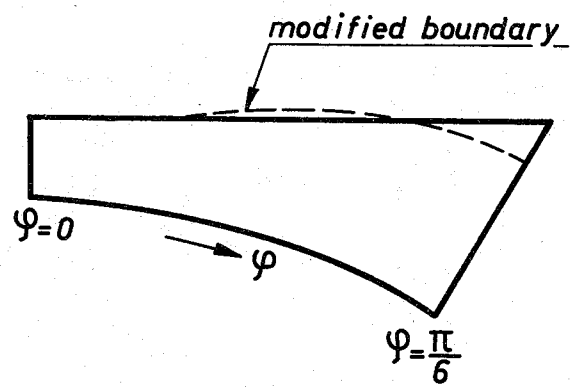


Fig.2 Nijsing's modified channel-element

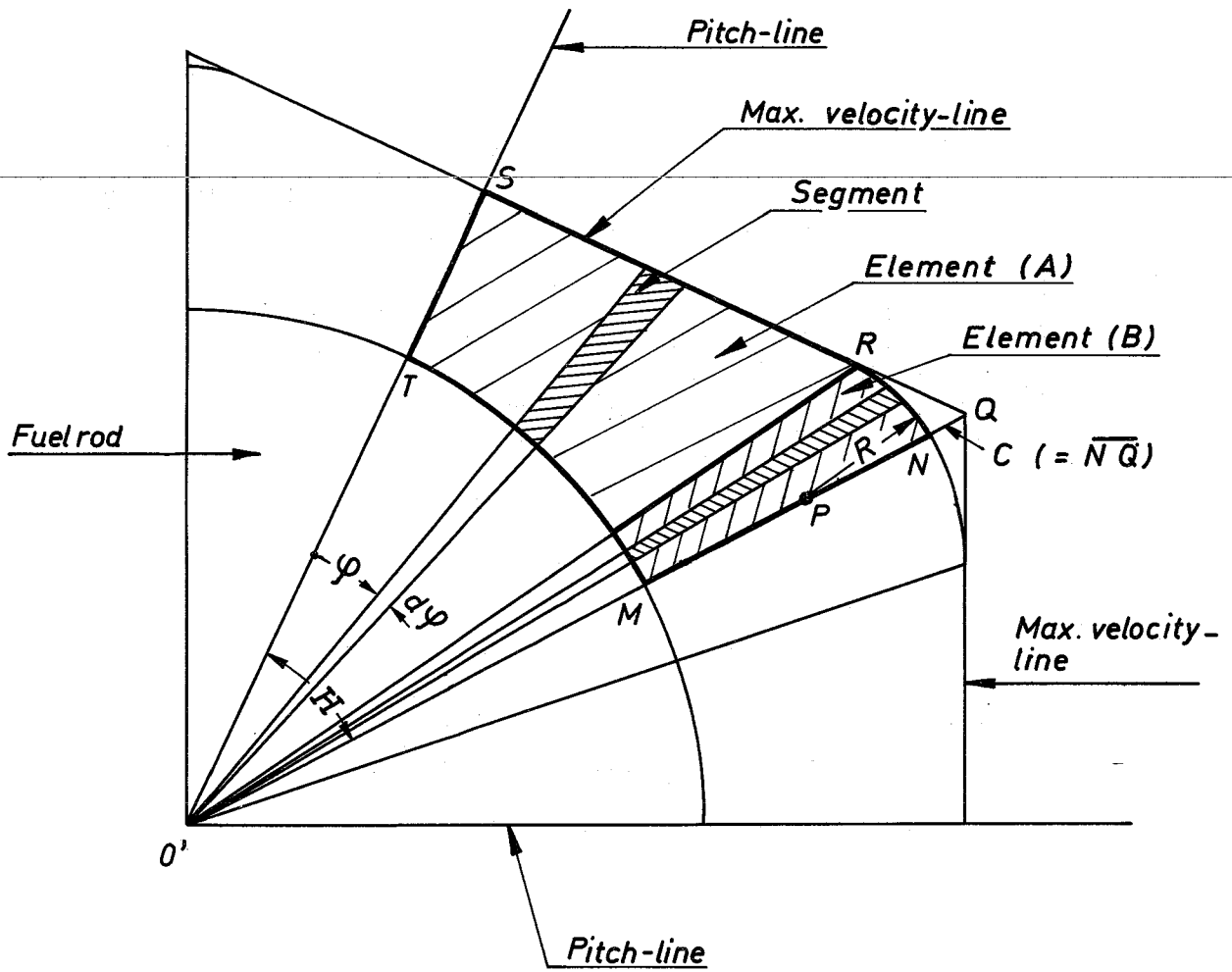


Fig.3 Definition of channel-element and segment used in the present analysis

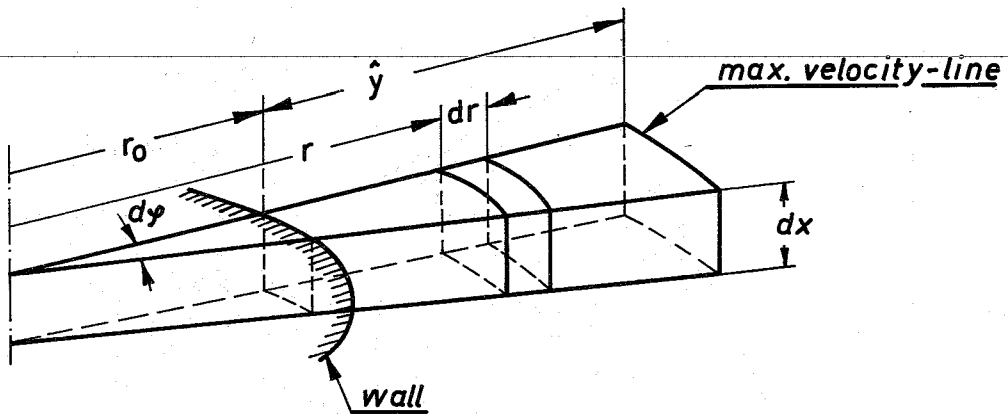


Fig.4 Coolant volume element in a cylindrical coordinate system

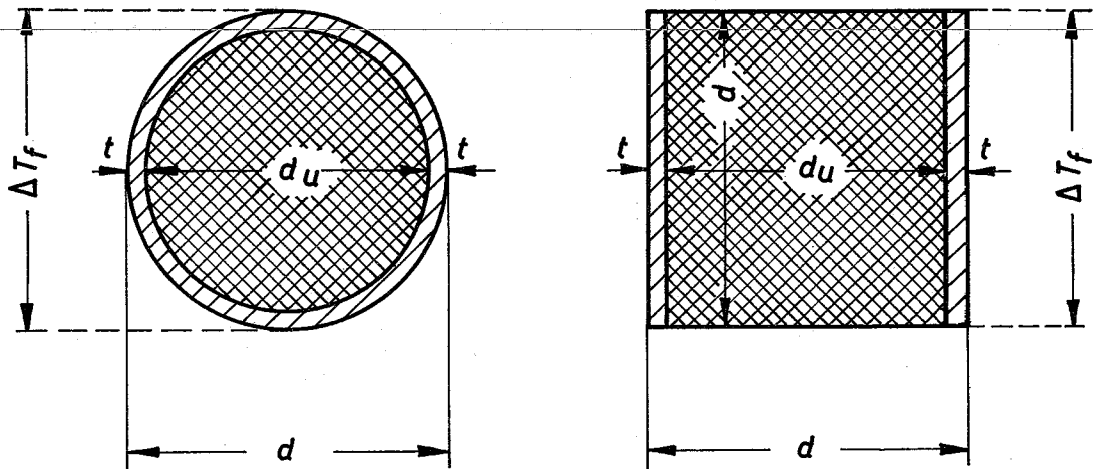


Fig.5 Simplified model on the right side to estimate the heat flow in the fuel and the cladding of the rod (on the left side) as a first approximation

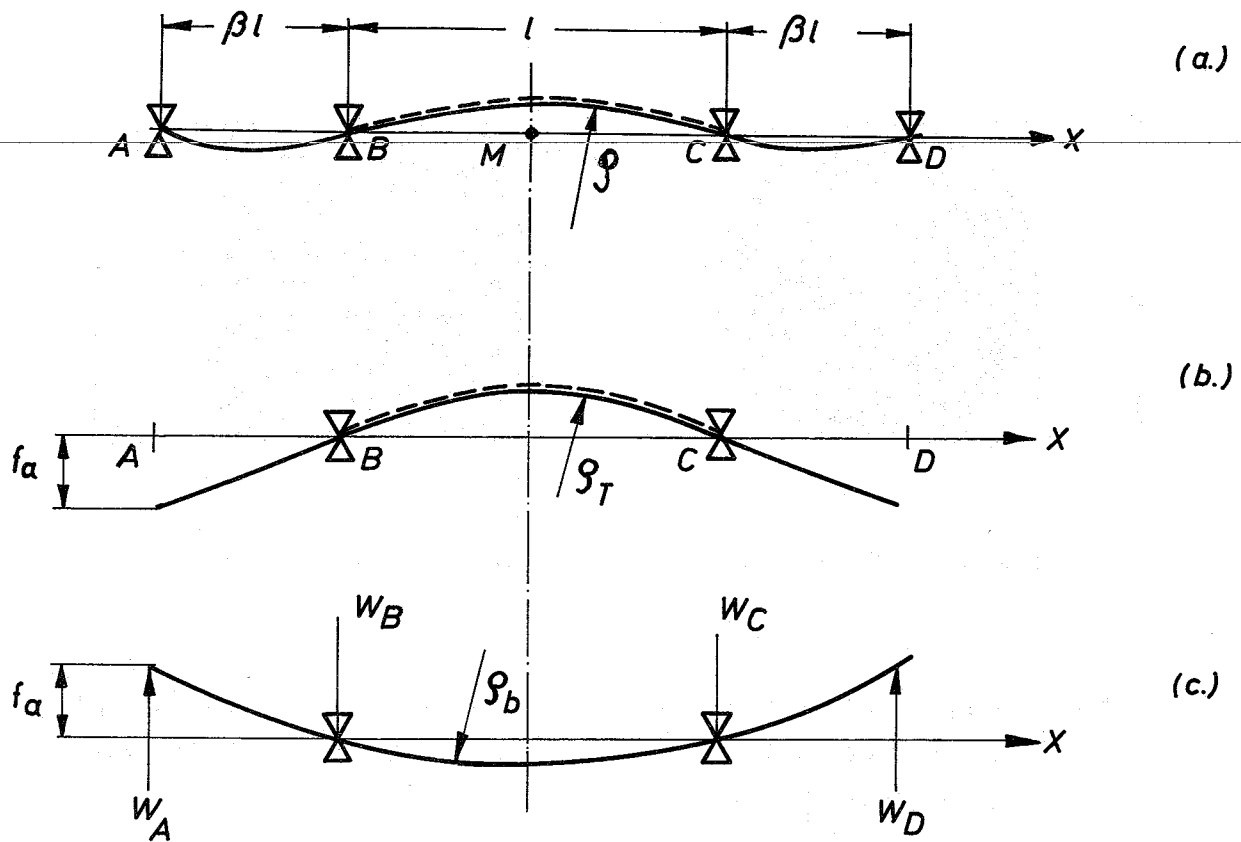


Fig.6 Bending curve of a fuel rod supported at four points

- a. The resultant bending curve
- b. Bending curve of the fuel rod supported at two points and exposed to a constant temperature difference ΔT_n between the two supports B and C
- c. Bending curve of the fuel rod loaded with restoring forces

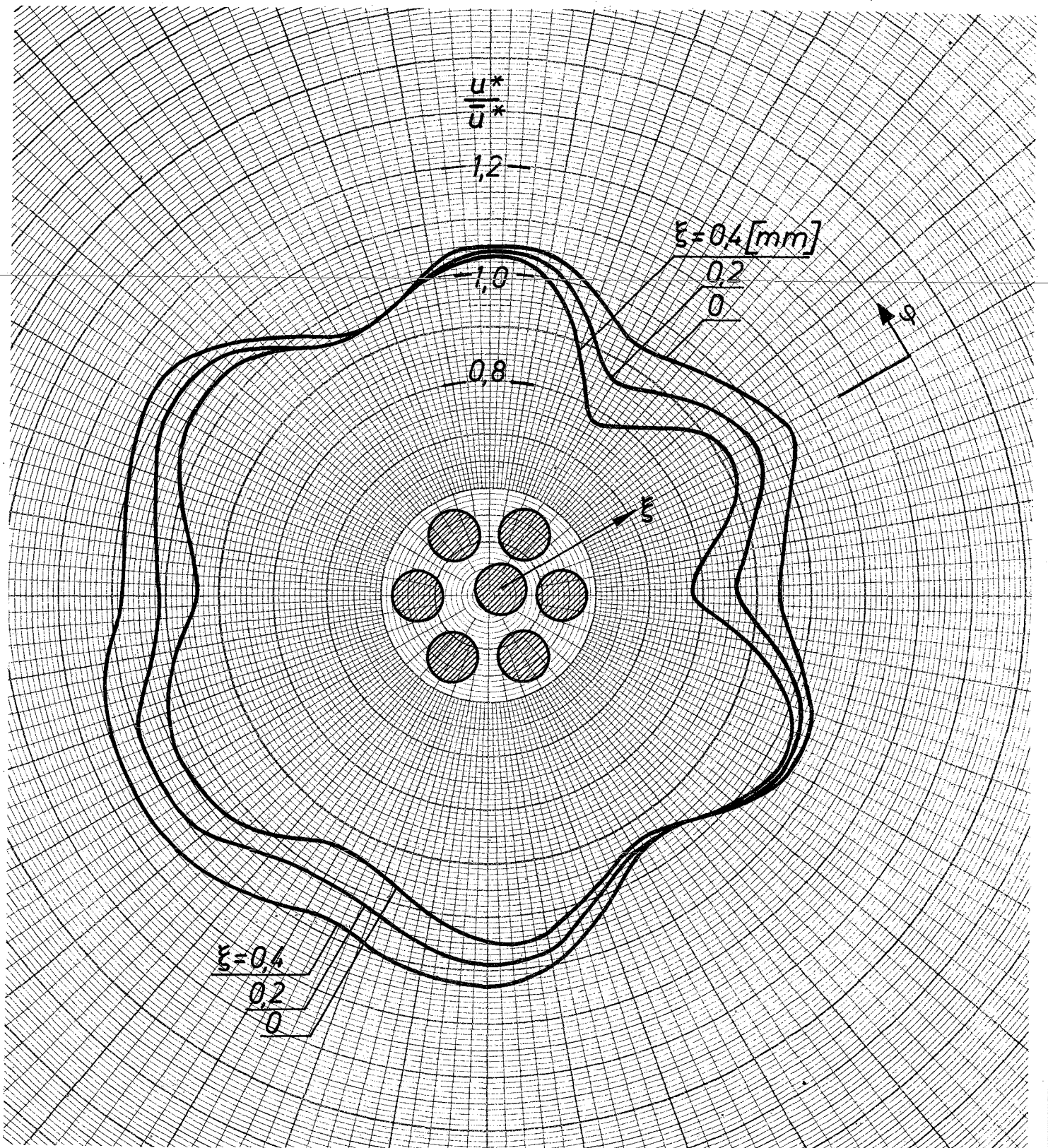


Fig.7 Friction velocity $\frac{u^*}{\bar{u}^*}$ vs angle φ

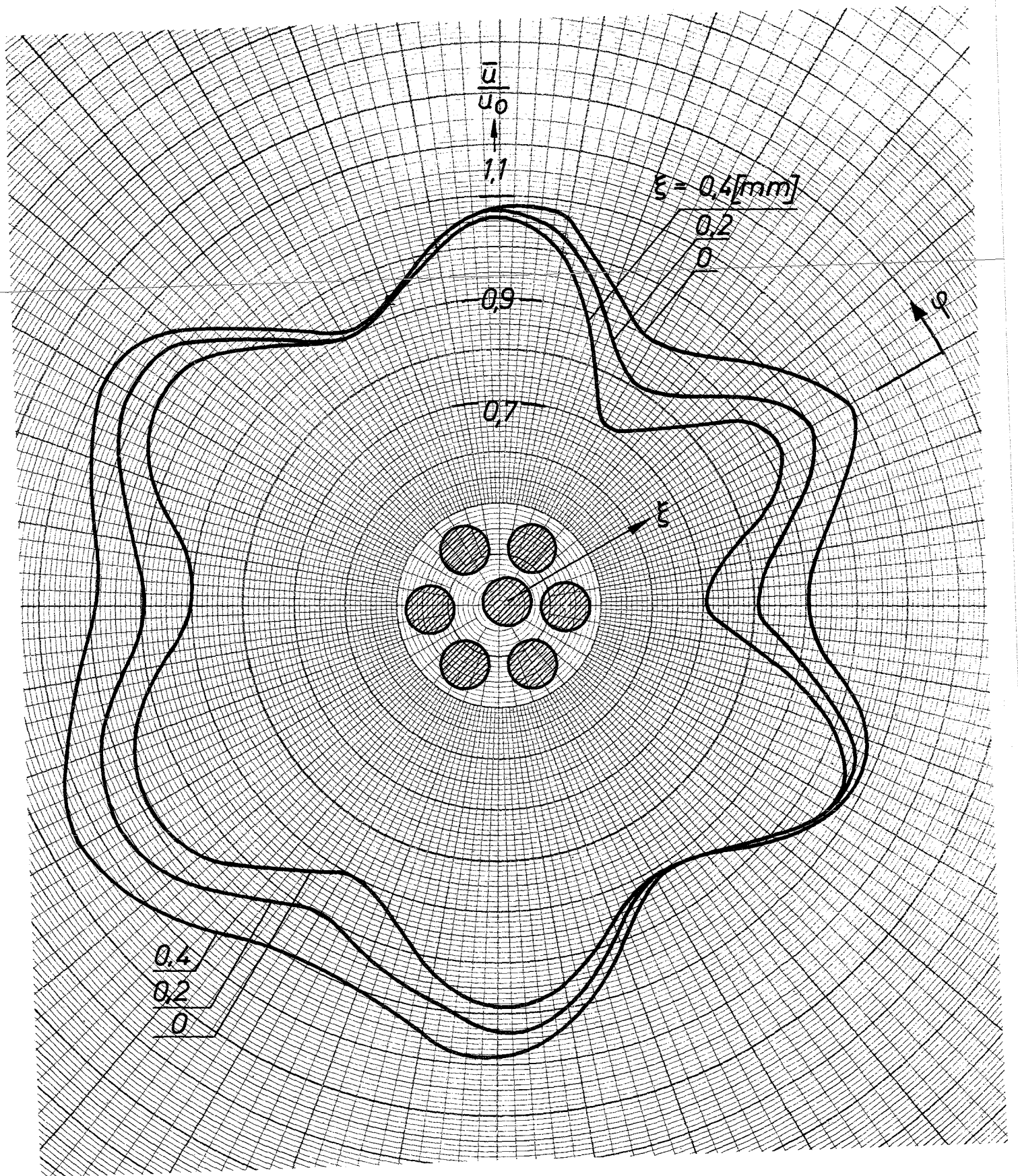


Fig.8 Flow velocity $\frac{\bar{u}}{u_0}$ vs angle φ

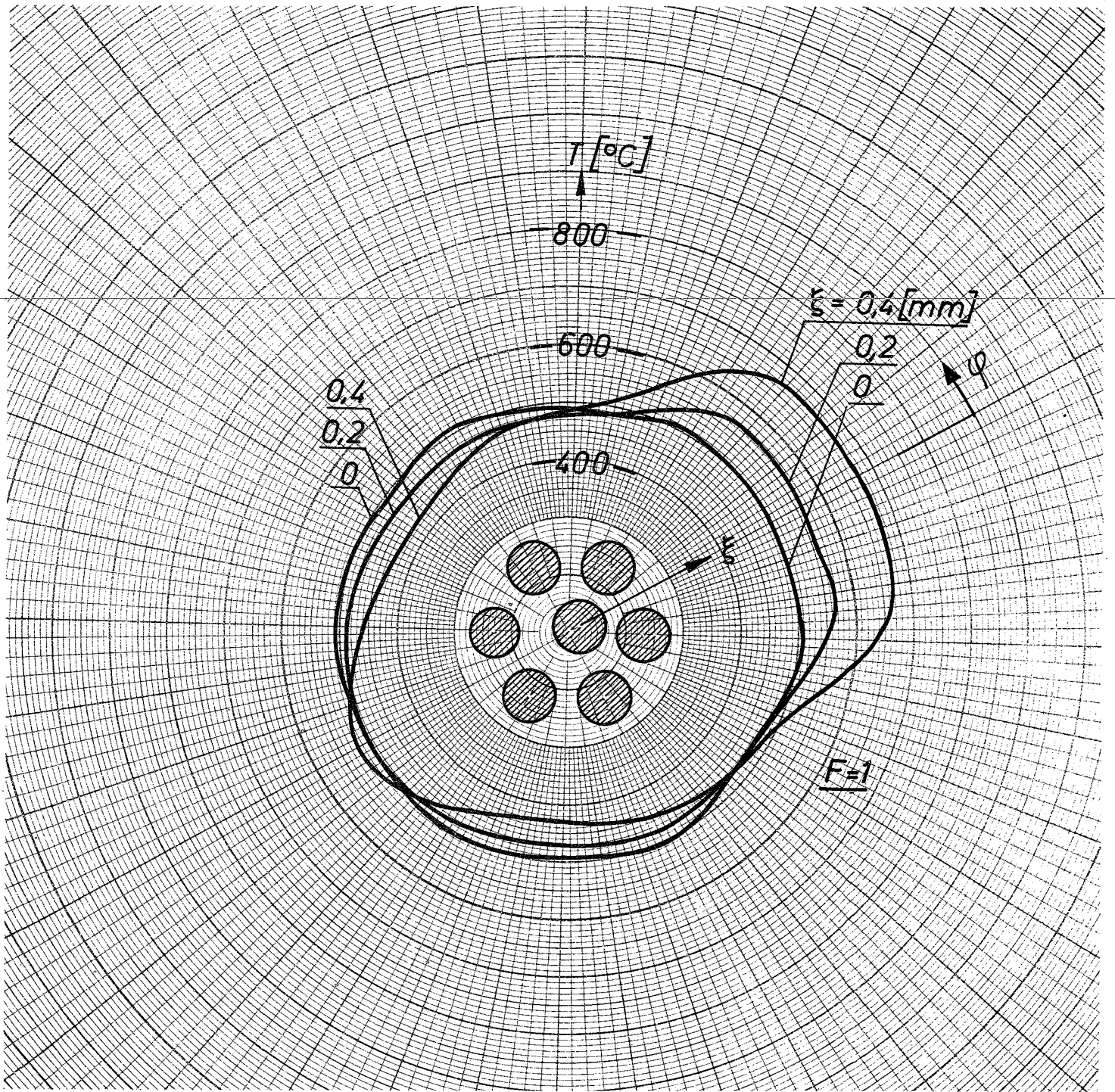


Fig.9 Coolant temperature T vs angle φ , $F = 1$

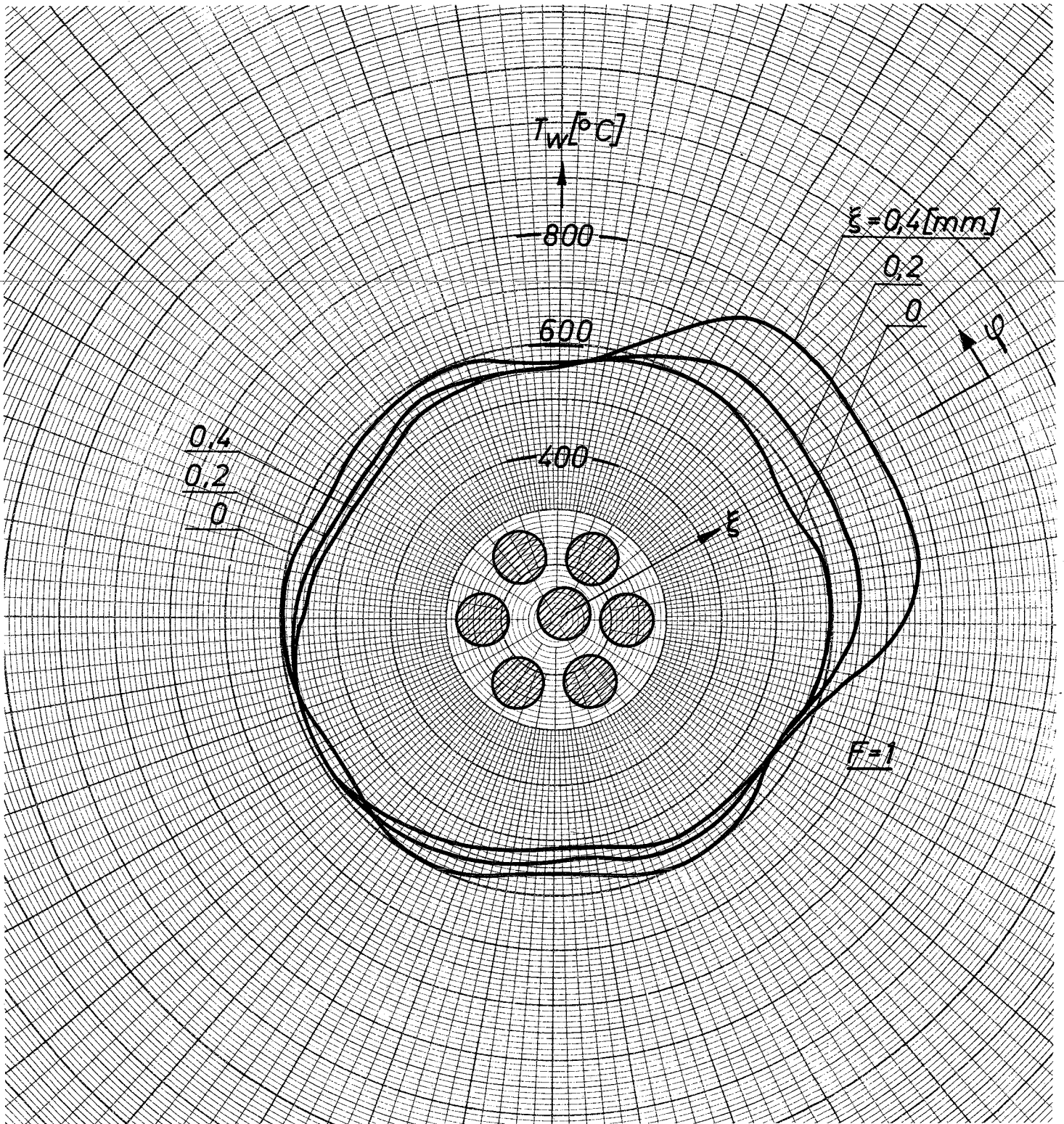


Fig.10 Clad surface temperature T_w vs angle φ , $F = 1$

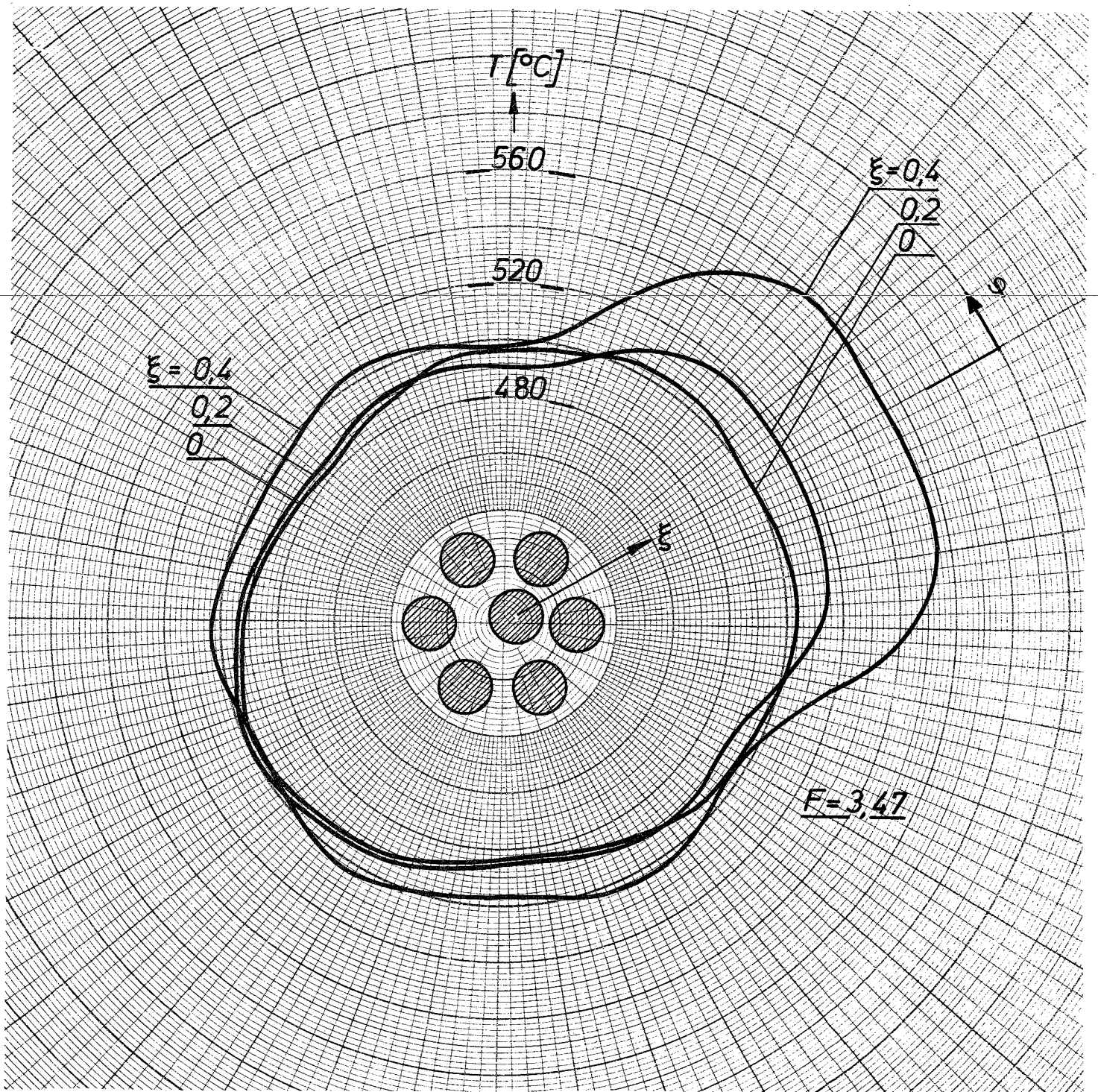


Fig.11 Coolant temperature T vs angle φ , $F = 3.47$

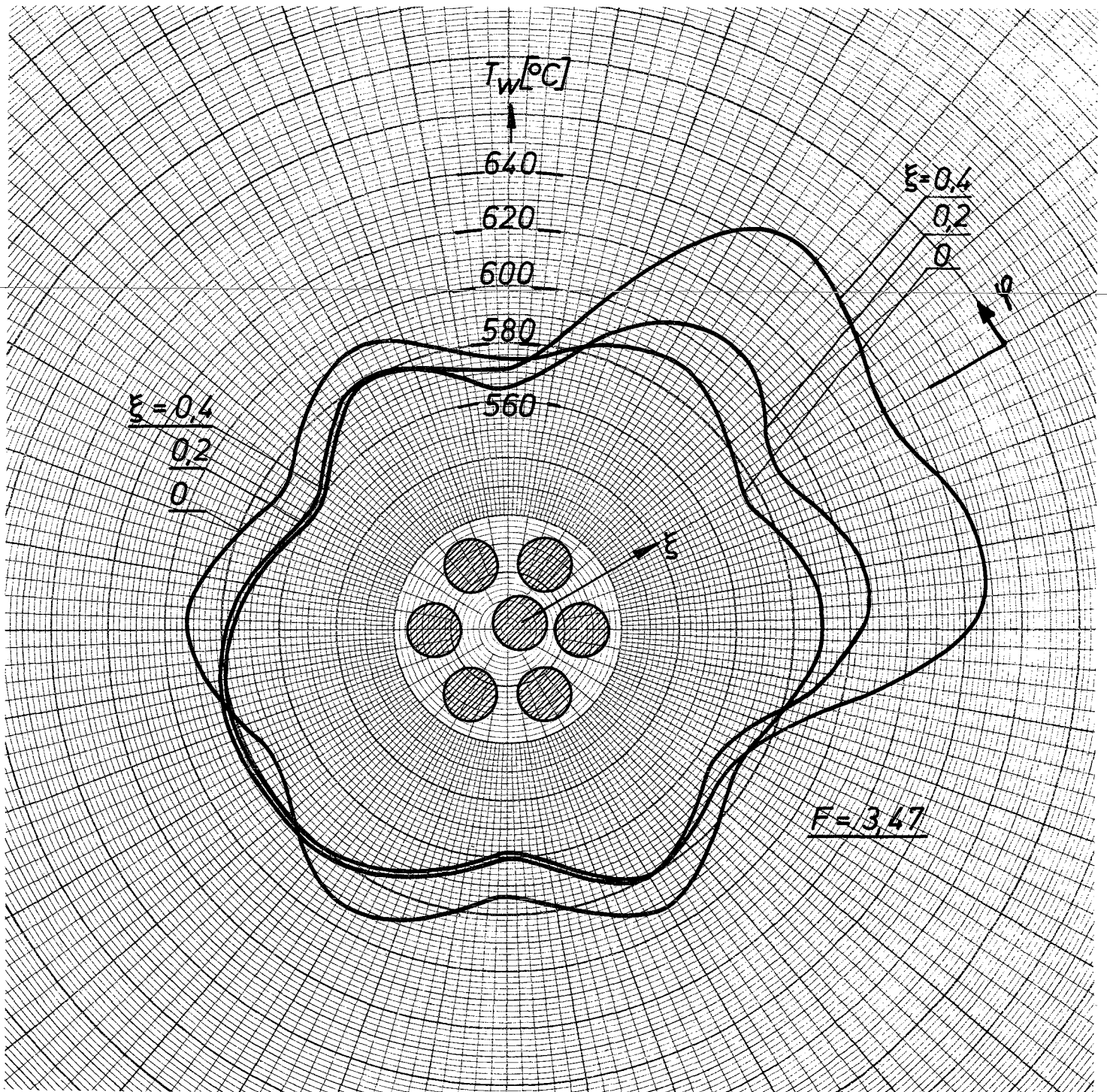


Fig.12 Clad surface temperature T_w vs angle φ , $F = 3.47$

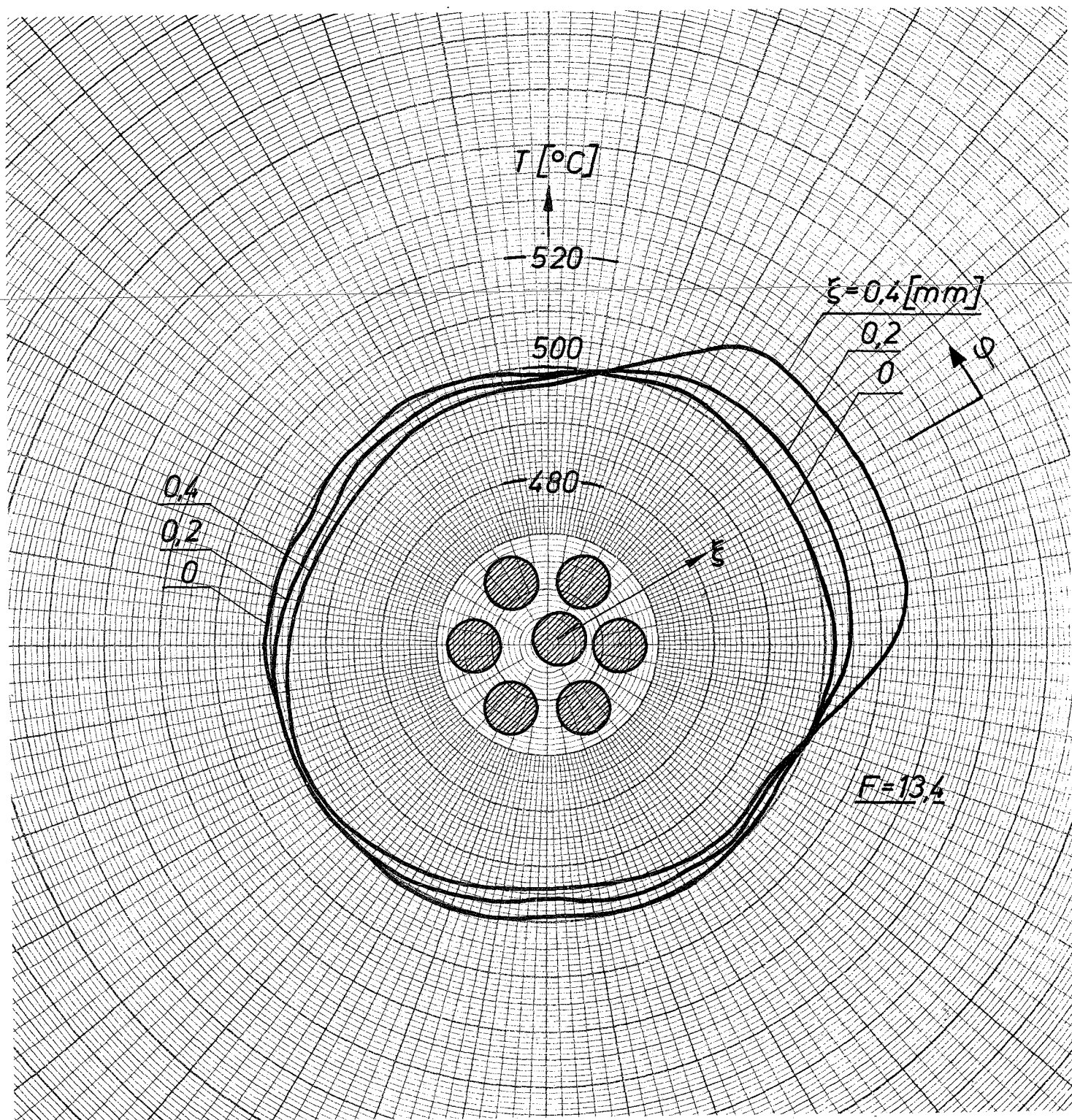


Fig.13 Coolant temperature T vs angle φ , $F = 13.4$

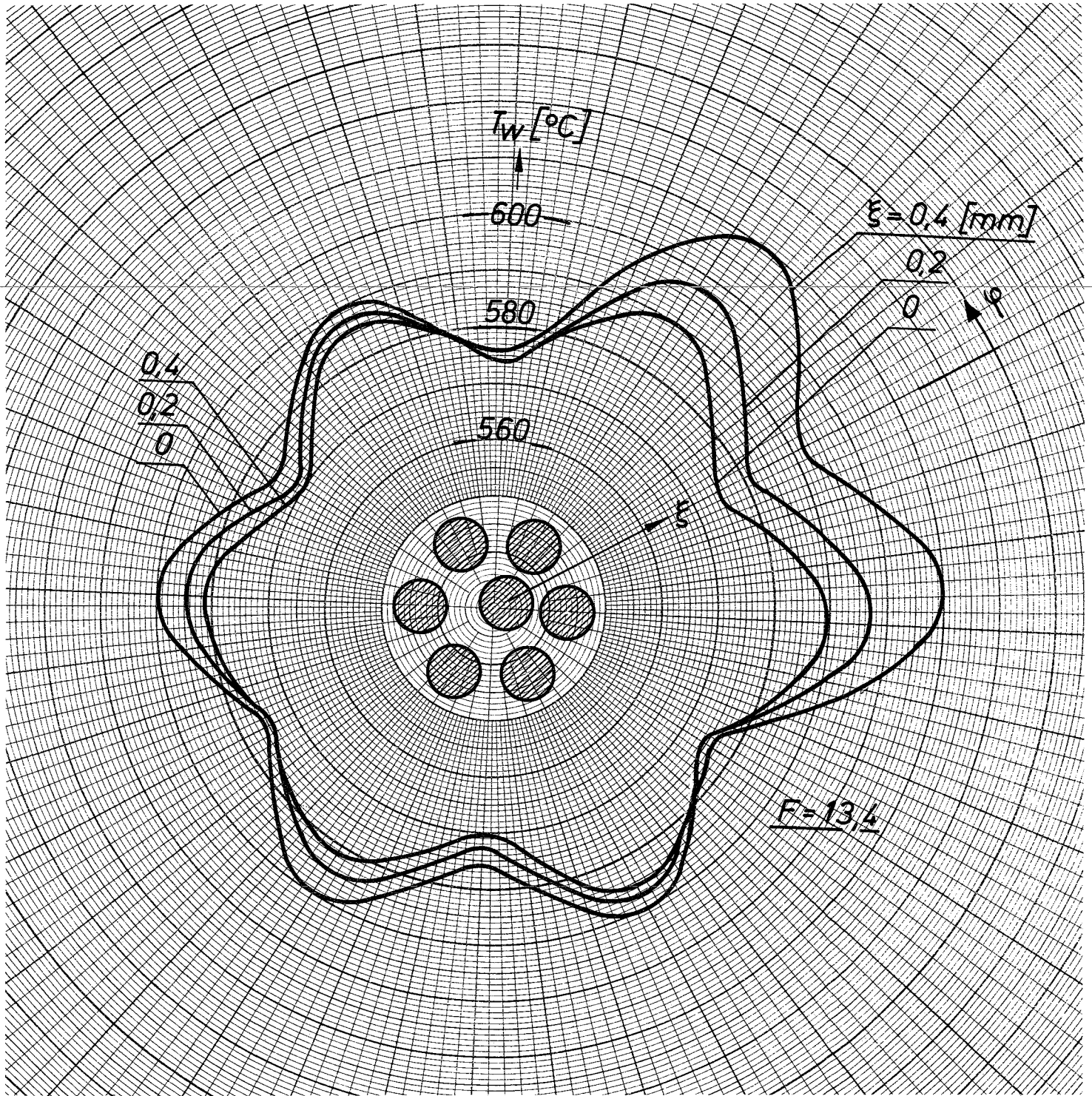


Fig.14 Clad surface temperature T_w vs angle ϕ , $F = 13.4$

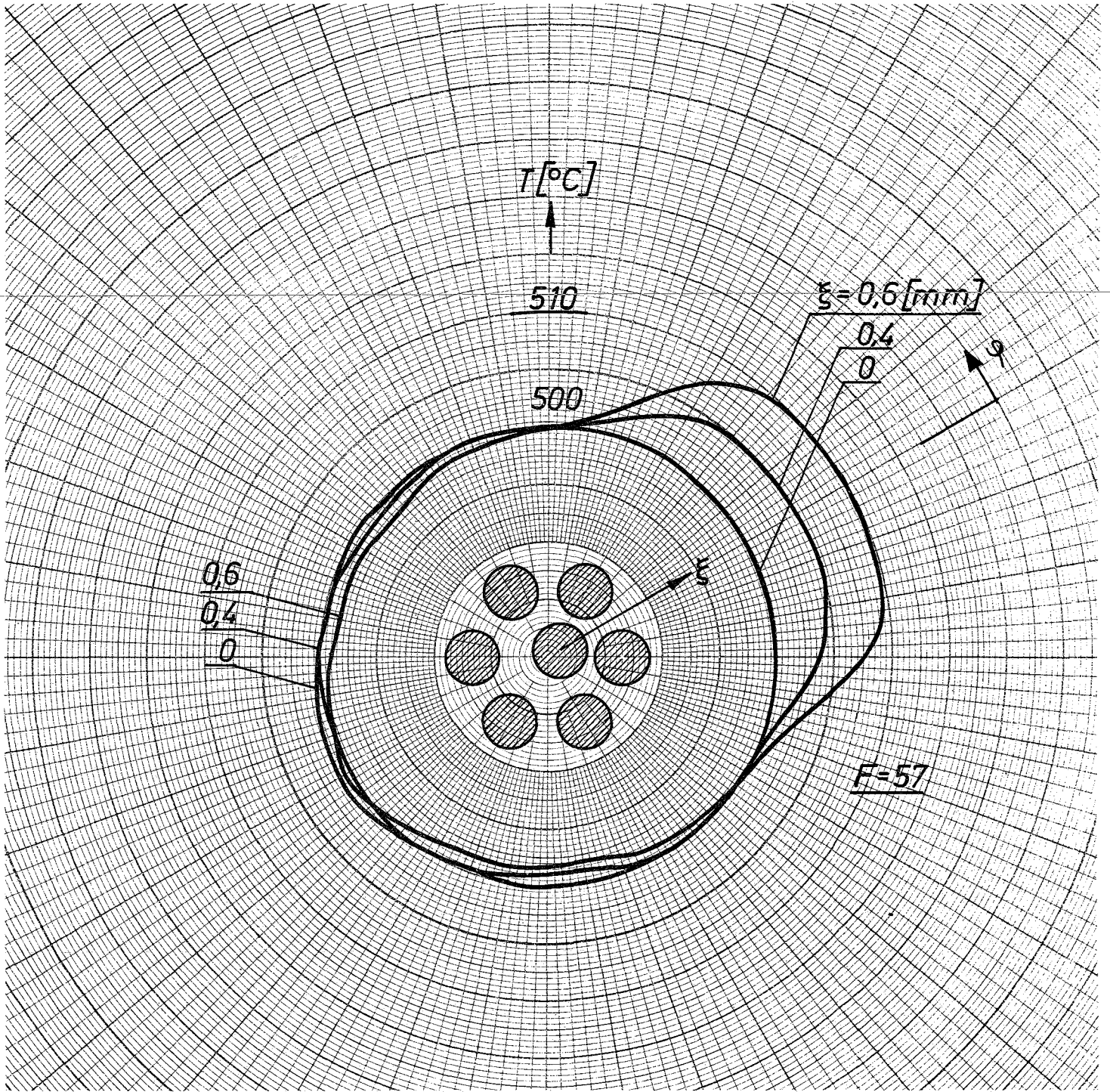


Fig.15 Coolant temperature T vs angle φ , $F = 57$

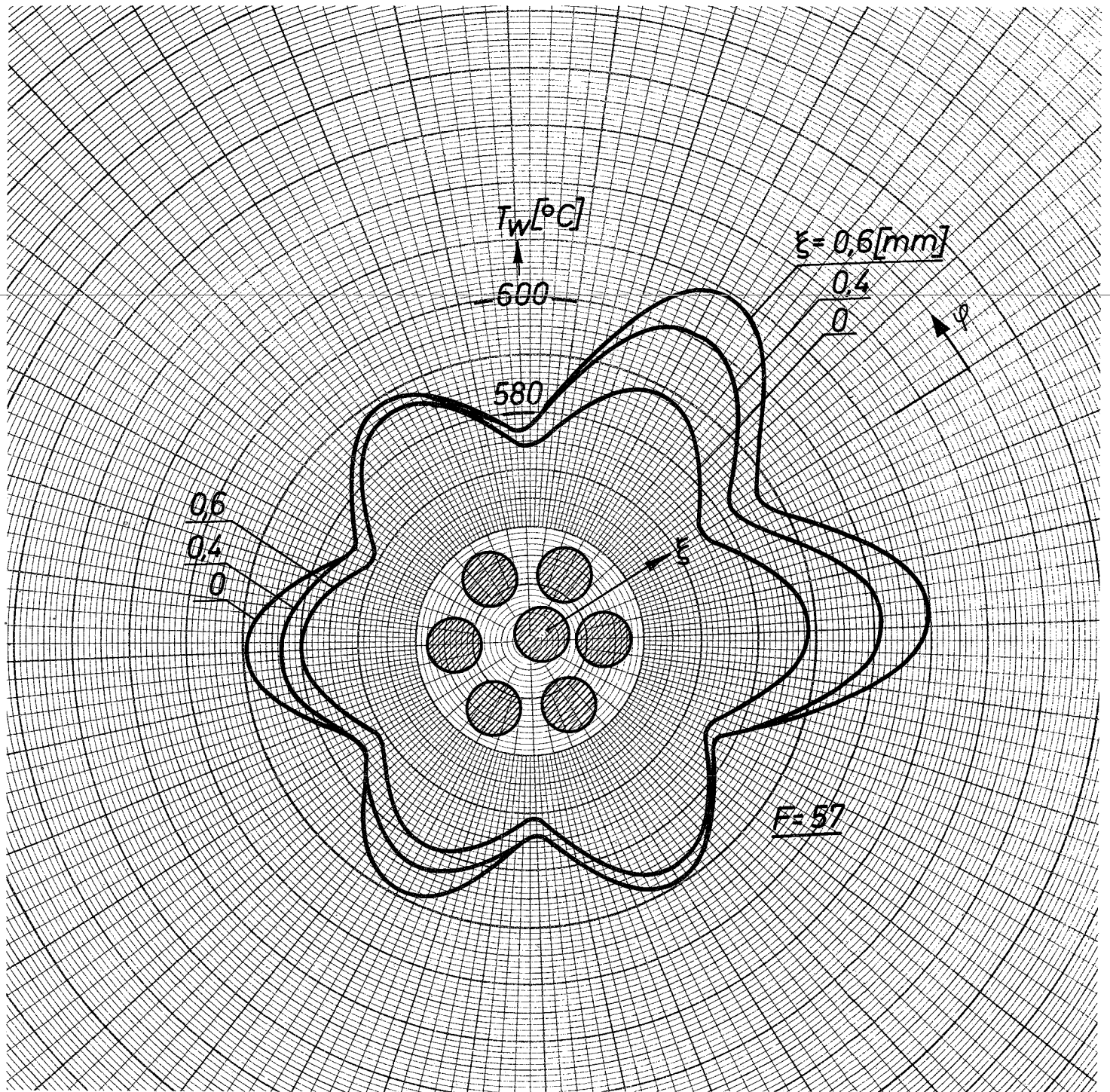


Fig.16 Clad surface temperature T_w vs angle φ , $F = 57$

- ΔT_w : Max.existing wall temperature difference around the deviated fuel rod
- - - ΔT_n : Critical temperature difference necessary to induce the specified deviating length for the given supporting length

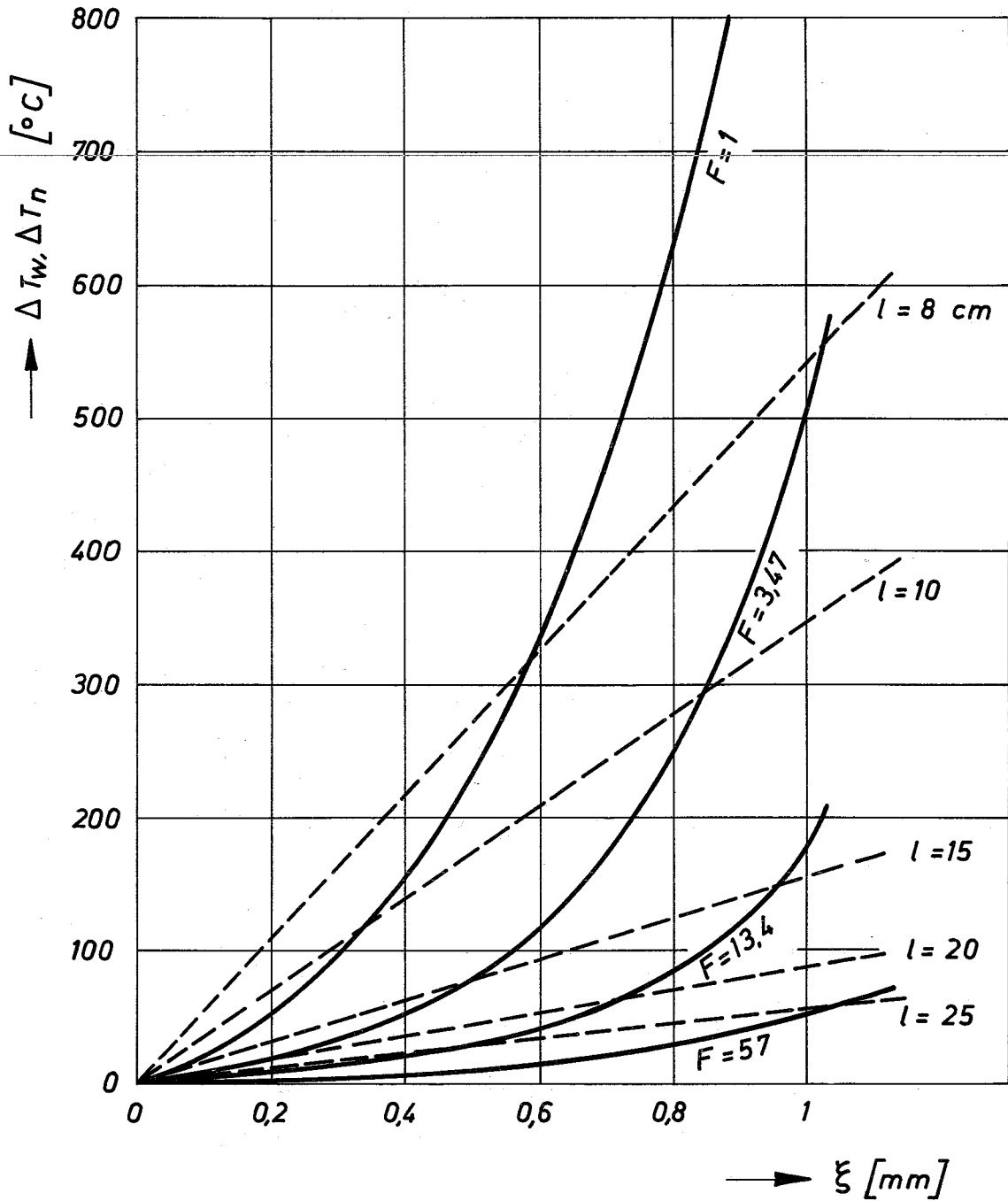


Fig.17 Max.existing and critical temperature differences ΔT_w , ΔT_n at the rod circumference as a function of deviation ξ at various supporting lengths l and F-values

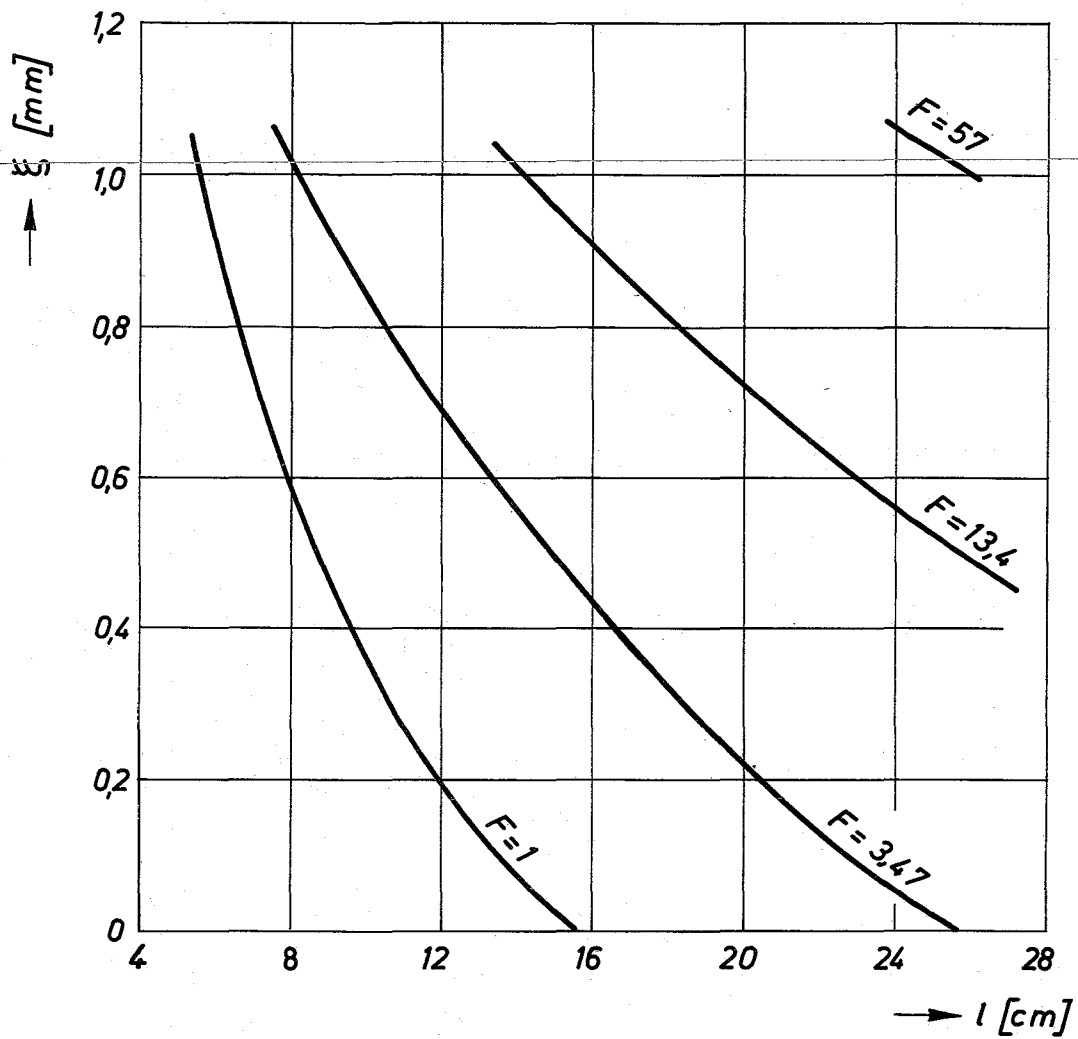


Fig.18 Stability limits as function of deviation ξ and supporting distance l at various F-values